Journal of Theoretical Biology 441 (2018) 68–83

Contents lists available at ScienceDirect

Journal of Theoretical Biology

journal homepage: www.elsevier.com/locate/jtbi

Deterministic stability regimes and noise-induced quasistable behavior in a pair of reciprocally inhibitory neurons

Mainak Patel[a,*], Badal Joshi[b]

[a] Department of Mathematics, College of William and Mary, United States
[b] Department of Mathematics, California State University San Marcos, United States

ARTICLE INFO

Article history:
Received 21 June 2017
Revised 24 November 2017
Accepted 11 December 2017
Available online 9 January 2018

ABSTRACT

Reciprocal inhibition is a common motif exploited by neuronal networks; an intuitive and tractable way to examine the behaviors produced by reciprocal inhibition is to consider a pair of neurons that synaptically inhibit each other and receive constant or noisy excitatory driving currents. In this work, we examine reciprocal inhibition using two models (a voltage-based and a current-based integrate-and-fire model with instantaneous or temporally structured input), and we use analytic and computational tools to examine the bifurcations that occur and study the various possible monostable, bistable, and tristable regimes that can exist; we find that, depending on system parameters (and on choice of neuron model), there can exist up to 3 distinct monostable regimes (denoted M0, M1, M2), 3 distinct bistable regimes (denoted B, B1, B2), and a single tristable regime (denoted T). We also find that synaptic inhibition exerts *independent control* over the two neurons – inhibition from neuron 1 to neuron 2 governs the spiking behavior of neuron 2 but has no impact on the spiking behavior of neuron 1 (and vice versa). The excitatory driving current, however, does not exhibit this property – the excitatory current to neuron 1 affects the spiking behavior of *both* neurons 1 and 2 (as does the excitatory current to neuron 2). Furthermore, we develop a methodology to examine the behavior of the system when the excitatory driving currents are allowed to be noisy, and we investigate the relationship between the behavior of the noisy system with the stability regime of the corresponding deterministic system.

1. Introduction

Reciprocal inhibition is an architectural motif commonly employed by the brain in a diverse array of computational tasks. For example, the reciprocal inhibition architecture arises in neural systems that underlie animal locomotion (Friesen, 1994), sleep-wake cycling (Hobson et al., 1975), REM-non REM sleep switching (Lu et al., 2006), binocular rivalry (Seely and Chow, 2011), and visual stimulus selection (Mysore and Knudsen, 2012). A detailed study of the dynamical behavior of mutually inhibitory neurons may therefore provide valuable insight into the computations performed by these various brain systems.

A mathematically tractable and intuitively transparent methodology for investigating reciprocal inhibition is to consider a simplified model of a pair of mutually inhibitory neurons, each of which receives an excitatory driving current (Fig. 1). Even such a simple dynamical system can exhibit a rich repertoire of dynamical behaviors. Depending on system parameters, the system may display one of two broad classes of steady-state behavior – the system can exhibit either monostability or bistability.

The dynamics of reciprocally connected inhibitory neurons, in the case that the parameters of synaptic inhibition are symmetric between the two cells, has been explored extensively in prior investigations. Mutually weak inhibition results in oscillatory spiking and a monostable system – both neurons fire in a periodic fashion, with the precise nature of the periodic behavior, and the spiking relationship between the two neurons, depending on the details of system parameters. Strong inhibition between a pair of symmetrically coupled neurons, on the other hand, can result in bistability – one neuron spikes at a fixed frequency while the other displays subthreshold oscillations for all time, with the identities of the active and suppressed cells determined by the initial conditions. Thus, one stable state consists of the first neuron firing with the second neuron silent, and the other stable state consists of the second neuron firing with the first neuron silent (Elson et al., 2001; Jalil et al., 2010; Kirillov et al., 1993; Rowat and Selverston, 1997; Skinner et al., 1994; Terman et al., 1998; Van Vreeswijk et al., 1994; Wang and Rinzel, 1992).

* Corresponding author.
E-mail address: mjpatel@wm.edu (M. Patel).

https://doi.org/10.1016/j.jtbi.2017.12.011
0022-5193/

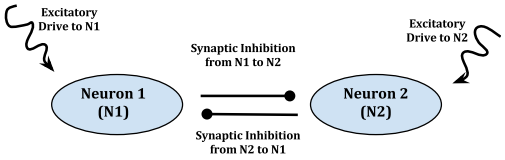

Fig. 1. Schematic of the dynamical system. The system consists of two mutually inhibitory neurons, each of which receives a constant excitatory driving current.

However, the transition from monostability to bistability as system parameters are varied, and the nature of the existing stable state(s), has not, to our knowledge, yet received a thorough theoretical investigation in the case that asymmetric coupling between the two mutually inhibitory neurons is allowed. In this work, we provide analytical and computational results on the existence of monostability versus bistability and the nature of the stable state(s) present as system parameters are varied in a pair of reciprocally inhibitory neurons in which asymmetry is permitted in all system parameters. Furthermore, in a deterministically bistable system, the addition of noise to the excitatory driving currents yields alternating bouts of spiking activity (Patel and Joshi, 2014), while in a monostable system noisy excitation results in two neurons that spike concurrently; we therefore also provide a methodology for assessing in a noisy system whether or not alternating activity bouts are occurring.

In the deterministic setting, when each neuron is capable of spiking continuously when uncoupled, there are three distinct modes of behavior that the coupled system can exhibit: after possibly a finite amount of time has passed: (0) both neuron 1 and neuron 2 actively spike for all time, (1) neuron 1 is active and neuron 2 is quiescent for all time, (2) same as (1) with the roles of neurons 1 and 2 switched. If a behavioral mode persists under a perturbation, we will refer to it as a stable mode. It is to be noted that a stable mode may correspond to multiple stable solutions of the dynamical system – for instance, in the stable mode (0) when the two neurons are simultaneously active, there might be two distinct stable solutions corresponding to distinct phase differences in the spike times of the two neurons. Thus, a stable mode (0), (1), or (2) is a set of one or more stable solutions with the prescribed property, instead of a single solution of the dynamical system. For a fixed set of parameters such that the neurons spike continuously when uncoupled, one or more of the three possible stable modes may exist, and the system will converge to a solution in one of the available modes depending on the initial conditions. When only one stable mode is available, we say that the set of parameters is in the monostable regime – M0, M1, or M2 – depending on which of the three modes is available, respectively. When two of the three modes are available, we say the system is in a bistable regime, and when all three modes are available, we say that the system is tristable. We emphasize that when we refer to the system as being in a monostable, bistable, or tristable regime, we are referring to the number of stable *modes* available, *not* necessarily to the number of stable *solutions* available. This is because, as discussed above, the stable mode (0) may in fact correspond to more than one stable solution of the dynamical system (the stable modes (1) and (2), on the other hand, each always correspond to a single stable solution).

We will employ two neuron models to describe our pair of reciprocally inhibitory neurons. In the first model, which we refer to as the voltage-based integrate-and-fire model (Stein, 1965), an incoming inhibitory spike has the effect of causing an instantaneous jump in the membrane potential from V to $V-\rho$ $(\rho>0)$, while in the second model, which we refer to as the current-based integrate-and-fire model, the effect of an incoming inhibitory spike is to cause a change in $\dot{V}$ in the form of a rectangular pulse. Thus, in the first model, the subthreshold membrane potential V has a discontinuity when the other neuron spikes and inputs are instantaneous, while in the second model subthreshold V is continuous but $\dot{V}$ has a discontinuity and inputs are temporally structured. While the voltage-based integrate-and-fire model is more amenable to a thorough mathematical treatment, the current-based integrate-and-fire model provides a more realistic representation of synaptic input (since synaptic inputs are temporally structured). We describe and analyze each model in detail, and we show that temporal structuring of synaptic input has a significant qualitative impact on the range of dynamical behaviors available to the two-neuron system. In particular, we find that temporally structured synaptic input (as opposed to modeling of synaptic input as instantaneous) expands the number of stable modes that the two neurons can exhibit within a parameter regime, suggesting that synaptic temporal dynamics can have a significant impact on the dynamical behaviors of a network. Finally, using the current-based integrate-and-fire model, we develop a methodology to assess the existence of alternating activity bouts in the two-neuron system in the case that external inputs to the two neurons are permitted to be noisy, and we discuss the application of this to the investigation of sleep-wake cycling behavior in infant mammals.

2. Stability regimes

In this paper, we study the dynamics of two neurons that are mutually inhibiting; each of these neurons receives enough external excitation to fire actively for all time, when uncoupled. Given such a model, with fixed set of parameters and initial conditions within the model, we are interested in determining the range of dynamical behaviors. Possibly after an initial transient lasting for a finite time, either (i) one of the two neurons fires actively for all time while the other neuron is quiescent for all time, or (ii) both neurons fire actively for all time. The main goal of this paper is to elucidate the different behaviors within a model as system parameters and initial conditions are varied. Specifically, we show that the set of available dynamical behaviors are different between a voltage-based integrate-and-fire model and a current-based integrate-and-fire model, with the latter exhibiting a much wider range of behaviors owing to the time course of inhibition that is present in the latter model but not in the former.

Consider the case where all the parameter values within the model are fixed. The spiking dynamics of the two neurons are completely determined within an integrate-and-fire model by the pair of voltages $(V_1(t), V_2(t))$. Suppose that the allowed set of initial conditions for the pair of voltages is $\mathcal{I}\subseteq\mathbb{R}^2$, i.e. $(v_1,v_2):=(V_1(0),V_2(0))\in\mathcal{I}$. Then we can partition $\mathcal{I}$ based on the eventual dynamics of the system starting at the point (v_1, v_2) as follows. If neuron i is eventually quiescent, possibly after firing a finite number of times, then we let $(v_1,v_2)\in\mathcal{Q}_i$. On the other hand, if neuron i is not eventually quiescent, we say that $(v_1,v_2)\in\mathcal{Q}_i^c=\mathcal{I}\setminus\mathcal{Q}_i$. Every initial voltage (v_1, v_2) belongs to one and only one of the following sets: $\mathcal{Q}_1\cap\mathcal{Q}_2$, $\mathcal{Q}_1\cap\mathcal{Q}_2^c$, $\mathcal{Q}_1^c\cap\mathcal{Q}_2$, and $\mathcal{Q}_1^c\cap\mathcal{Q}_2^c$. In fact, since we are assuming for all models under study that both neurons receive enough excitation to spike when uncoupled, $\mathcal{Q}_1\cap\mathcal{Q}_2$ is empty for all parameter values. This is because when both neurons are quiescent, the system is effectively uncoupled since no inhibition is being sent from one neuron to another and so one of the two neurons must spike eventually. Thus for any given set of parameters, there exist at most three distinct available *modes*: $\mathcal{Q}_1\cap\mathcal{Q}_2^c$, $\mathcal{Q}_1^c\cap\mathcal{Q}_2$, and $\mathcal{Q}_1^c\cap\mathcal{Q}_2^c$, i.e. the set of initial conditions $\mathcal{I}$ is partitioned into $\mathcal{Q}_1\cap\mathcal{Q}_2^c$, $\mathcal{Q}_1^c\cap\mathcal{Q}_2$, and $\mathcal{Q}_1^c\cap\mathcal{Q}_2^c$. Furthermore, we say that a mode is stable if it contains an open disk in $\mathbb{R}^2$.

A point in parameter space is said to belong to one of the *regimes* $M0$, $M1$, $M2$, B, $B1$, $B2$, or T depending on which modes

are nonempty (i.e. available) and are stable. We give below a description of each of these regimes.

1. Monostable regime $M0$: the set of stable modes is $\{\mathcal{Q}_1^c \cap \mathcal{Q}_2^c\}$. For all initial conditions, both neurons are active for all time.
2. Monostable regime $M1$: the set of stable modes is $\{\mathcal{Q}_1^c \cap \mathcal{Q}_2\}$. For all initial conditions, neuron 1 is active for all time while neuron 2 is quiescent for all time (after possibly firing finitely many spikes).
3. Monostable regime $M2$: the set of stable modes is $\{\mathcal{Q}_1 \cap \mathcal{Q}_2^c\}$. For all initial conditions, neuron 2 is active for all time while neuron 1 is quiescent for all time (after possibly firing finitely many spikes).
4. Bistable regime B: the set of stable modes is $\{\mathcal{Q}_1^c \cap \mathcal{Q}_2, \mathcal{Q}_1 \cap \mathcal{Q}_2^c\}$. There exists a nonempty open disk of initial conditions which lead to neuron 1 active and neuron 2 quiescent for all time, there also exists a disjoint open disk of initial conditions which eventually leads to neuron 2 active and neuron 1 quiescent for all time, and there are no other stable modes.
5. Bistable regime $B1$: the set of stable modes is $\{\mathcal{Q}_1^c \cap \mathcal{Q}_2, \mathcal{Q}_1^c \cap \mathcal{Q}_2^c\}$. There exists a nonempty open disk of initial conditions which eventually leads to neuron 1 active and neuron 2 quiescent for all time, there also exists a disjoint open disk of initial conditions which lead to neurons 1 and 2 being simultaneously active for all time, and there are no other stable modes.
6. Bistable regime $B2$: the set of stable modes is $\{\mathcal{Q}_1 \cap \mathcal{Q}_2^c, \mathcal{Q}_1^c \cap \mathcal{Q}_2^c\}$. There exists a nonempty open disk of initial conditions which lead to neuron 2 active and neuron 1 quiescent for all time, there also exists a disjoint open disk of initial conditions which lead to neurons 1 and 2 being simultaneously active for all time, and there are no other stable modes.
7. Tristable regime T: the set of stable modes is $\{\mathcal{Q}_1^c \cap \mathcal{Q}_2, \mathcal{Q}_1 \cap \mathcal{Q}_2^c, \mathcal{Q}_1^c \cap \mathcal{Q}_2^c\}$. There exist three disjoint nonempty open disks of initial conditions, one leads to neuron 1 active and neuron 2 quiescent for all time, another to neuron 2 active and neuron 1 quiescent for all time, a third to both neurons firing actively for all time, and there are no other stable modes.

3. Voltage-based I&F Model

For $i, j \in \{1, 2\}$ such that $i \neq j$, the dynamics for the subthreshold membrane potential of a pair of voltage-based integrate-and-fire neurons (Stein, 1965) that mutually inhibit each other is given by

$$\begin{aligned} &\dot{V}_i = -gV_i + \alpha_i \\ &(V_i(t) = 1 \text{ and } V_j(t) < 1) \Rightarrow (V_i(t^+) = 0,\ V_j(t^+) = V_j(t) - \rho_i) \\ &(V_1(t) = 1 \text{ and } V_2(t) = 1) \Rightarrow ((V_1(t^+), V_1(t^+)) = (-\rho_2, -\rho_1)) \end{aligned} \tag{1}$$

where initial voltages are assumed to be $V_1(0) \leq 1$, $V_2(0) \leq 1$. Here g is the synaptic conductance and α_i is a constant excitatory current applied to neuron i. When the membrane potential V_i of neuron i reaches the spiking threshold of 1, it is immediately reset to 0, and we say that neuron i spikes at that time. We assume that $\alpha_i > g$ so that in the absence of inhibition, each neuron is actively spiking with a period of $T_i = -\ln(1 - g/\alpha_i)/g$. $\rho_i > 0$ is the strength of inhibition from neuron i to neuron j. When neuron j spikes, the other neuron $i \neq j$ receives an inhibitory impulse and its membrane potential jumps down by an amount ρ_j. When both neurons spike together, we assume that both neurons are reset to 0 and they both receive an inhibitory impulse from the other neuron. In other words, immediately after the simultaneous spikes, the membrane potentials are reset to $(V_1, V_2) = (-\rho_2, -\rho_1)$.

Let $t_0, t_1, t_2, \ldots$ be the sequence of spiking times; in other words, at time t_k one of the two neurons (or both neurons) spike. In this model, the jumps in V_i are downward only, since all jumps arise from either an inhibitory impulse or from reset to $V_i = 0$ after neuron i has spiked. From this observation, it is clear that for all initial conditions $V_1(0) \leq 1$, $V_2(0) \leq 1$, it is the case that $V_1(t) \leq 1$, $V_2(t) \leq 1$ for all time $t \geq 0$. Thus, for some $w < 1$, the pair of membrane potentials of the two neurons at each spike time t_k takes one of the following forms:

$$(V_1(t_k), V_2(t_k)) = \begin{cases} (w, 1) & \text{if neuron 2 spikes at time } t_k, \\ (1, w) & \text{if neuron 1 spikes at time } t_k, \\ (1, 1) & \text{if both neurons spike at time } t_k. \end{cases}$$

We show in this section that the only stable modes for model (1) are M0, M1, M2, and B. The main result of this section, Theorem 3.9, characterizes the suite of possible behaviors including the precise dependence on parameter values.

We define the two-dimensional Poincare map to be the pair of membrane potentials at the spike times $t_k \mapsto \mathbf{v}_k := (V_1(t_k), V_2(t_k))$ for $k \in \{0, 1, 2, \ldots\}$. For instance, if at time t_k, neuron 2 spikes but not neuron 1 then the state of the system at this time is $\mathbf{v}_k = (V_1(t_k), V_2(t_k)) = (w_k, 1)$ with $w_k < 1$. More precisely, the Poincare map is defined as follows:

Definition 3.1. Let $(t_0, t_1, t_2, \ldots)$ be a sequence such that

1. $0 < t_0 < t_1 < t_2 < \ldots$.
2. $$\max(V_1(t), V_2(t)) \quad \begin{cases} = 1, & \text{if } t = t_k \\ < 1, & \text{if } t \neq t_k \end{cases}$$

We define the *system spike map* by $\mathbf{v}_k = (V_1(t_k), V_2(t_k))$ for $k = 0, 1, 2, \ldots$.

Definition 3.2. For $j \in \{1, 2\}$ such that $j \neq i$,

(i) define the *headstart phase for neuron i*, $\bar{w}_i$ to be

$$\bar{w}_i := \rho_j + \frac{1 - \alpha_i/\alpha_j}{1 - g/\alpha_j}$$

and,

(ii) define the *limiting phase for neuron i*, $w_{\infty,i}$ to be

$$w_{\infty,i} := \frac{\alpha_i}{g} + \rho_j\left(1 - \frac{\alpha_j}{g}\right).$$

Suppose at time t_k neuron 2 spikes but not neuron 1; Lemma 3.3 determines whether neuron 1 or neuron 2 will spike at time t_{k+1} based on the membrane potential of neuron 1 at time t_k.

Lemma 3.3. *If* $\mathbf{v}_k = (w, 1)$ *with*

$$w \begin{cases} < \bar{w}_1, & \textit{neuron 2 spikes but not neuron 1 at time } t_{k+1} \\ = \bar{w}_1, & \textit{both neurons spike at time } t_{k+1} \\ > \bar{w}_1, & \textit{neuron 1 spikes but not neuron 2 at time } t_{k+1} \end{cases}$$

Proof. Between spikes, both $V_1(t)$ and $V_2(t)$ are increasing functions that are solutions to autonomous differential equations. We only need to show that if $w = \bar{w}_1$, then both neurons reach the spiking threshold $V = 1$ at the same time. The subthreshold membrane potential for 2 in the time interval (t_k, t_{k+1}) is easily solved to be $V_2(t) = \frac{\alpha_2}{g}\left(1 - e^{-g(t-t_k)}\right)$. Similarly, we solve for the subthreshold membrane potential of 1 in the same time interval (t_k, t_{k+1}), $V_1(t) = \frac{1}{g}\left(\alpha_1 - (\alpha_1 - g(w - \rho_2))e^{-g(t-t_k)}\right) = \frac{\alpha_1}{\alpha_2}V_2(t) + (w - \rho_2)\left(1 - g\frac{V_2(t)}{\alpha_2}\right)$, where we rewrote $V_1(t)$ in terms of $V_2(t)$. For $w = \bar{w}_1$, we have

$$V_1(t) = \frac{\alpha_1}{\alpha_2}V_2(t) + \frac{1 - \alpha_1/\alpha_2}{1 - g/\alpha_2}\left(1 - g\frac{V_2(t)}{\alpha_2}\right)$$

For $\alpha_1 > g$, it is easy to see that $V_2 = 1$ if and only if $V_1 = 1$ in the above expression. □

We assume without loss of generality that neuron 2 spikes at time t_k and let $\mathbf{v}_k := (w_k, 1)$. First we consider the case $w_k < \bar{w}_1$, so that neuron 2 spikes again at time t_{k+1} and we let $\mathbf{v}_{k+1} := (w_{k+1}, 1)$. In the next lemma, we determine w_{k+1} as a function of w_k.

Lemma 3.4. *If $\mathbf{v}_k := (w_k, 1)$ with $w_k < \bar{w}_1$, then $\mathbf{v}_{k+1} = (w_{k+1}, 1)$ with*

$$w_{k+1} = \frac{\alpha_1}{\alpha_2} + (w_k - \rho_2)\left(1 - \frac{g}{\alpha_2}\right)$$

Proof. Since $w_k < \bar{w}_1$, neuron 2 will spike and neuron 1 will not spike at time t_{k+1}. We first find the time to spiking $t_{k+1} - t_k$ for neuron 2 by elementary integration. Then we calculate the sub-threshold membrane potential of neuron 1 at t_{k+1} by performing another simple integration over the time interval (t_k, t_{k+1}) with the initial condition $V_1(t_k) = w_k - \rho_2$. This immediately gives the stated result. □

The map $w_k \mapsto w_{k+1}$ appearing in Lemma 3.4 can be solved explicitly.

Lemma 3.5. *Consider the one-dimensional map defined by $w_{k+1} = \frac{\alpha_1}{\alpha_2} + (w_k - \rho_2)\left(1 - \frac{g}{\alpha_2}\right)$. Then for $n \in \mathbb{Z}_{\geq 0}$, $w_n = w_{\infty,1} + (w_0 - w_{\infty,1})\left(1 - \frac{g}{\alpha_2}\right)^n$.*

Proof. Since $w_{k+1} = f(w_k)$ is a linear map, it can be solved explicitly by summing a finite geometric series. □

The previous lemma provides the reason for naming $w_{\infty,i}$ as the limiting phase of neuron i. Suppose we start with the initial condition $\mathbf{v}_0 = (w_0, 1)$ with $w_0 < 1$. Let N be the smallest integer with the property that $w_N > \bar{w}_1$, then either the first N or $N-1$ spikes (depending on whether $w_N < 1$ or $w_N > 1$) will arise in neuron 2, and the following spike will arise in neuron 1. It is easy to see that w_n in the previous lemma is a monotone sequence converging to $w_{\infty,1}$. It follows then that if $w_{\infty,1} \leq \bar{w}_1$ then neuron 2 will remain actively spiking for all time while neuron 1 will remain quiescent for all time. On the other hand, if $w_{\infty,1} > \bar{w}_1$, then neuron 1 will fire a spike after a finite time interval. Let $\Gamma_{2,1} := \frac{\rho_2(\alpha_2 - g)}{\alpha_1 - g}$ and $\Gamma_{1,2} := \frac{\rho_1(\alpha_1 - g)}{\alpha_2 - g}$. We note that $\Gamma_{1,2}, \Gamma_{2,1} > 0$, since the excitatory currents satisfy $\alpha_1 > g$, $\alpha_2 > g$.

Proposition 3.6. *Suppose that neuron 2 fires and neuron 1 does not fire initially, so that $\mathbf{v}_0 = (w_0, 1)$ with $w_0 < 1$. Then neuron 1 will fire after a finite time interval if and only if $\rho_2 < \frac{\alpha_1 - g}{\alpha_2 - g}$ or equivalently $\Gamma_{1,2} < 1$.*

Proof. Neuron 1 will fire after a finite time interval if and only if the limiting phase of neuron 1 is strictly greater than the headstart phase of neuron 1, $w_{\infty,1} > \bar{w}_1$. The result follows on simplifying this condition. □

Proposition 3.6 states that if $\Gamma_{1,2} < 1$, then neuron 1 cannot be suppressed, irrespective of the initial conditions. Clearly $w_{\infty,1} > 1$ is sufficient for neuron 1 to spike after a finite time interval. The next result shows that this condition is necessary as well.

Lemma 3.7. *If $w_{\infty,i} > \bar{w}_i$ then $w_{\infty,i} > 1 > \bar{w}_i$. If $w_{\infty,i} < \bar{w}_i$ then $w_{\infty,i} < 1 < \bar{w}_i$.*

Proof. After some algebra, we write $\bar{w}_i$ as a function of $w_{\infty,i}$,

$$\bar{w}_i = \frac{\alpha_j - g w_{\infty,i}}{\alpha_j - g}$$

If $w_{\infty,i} < 1$ then $\bar{w}_i > 1$ and if $w_{\infty,i} > 1$ then $\bar{w}_i < 1$, from which the result follows: □

This shows that if initially neuron 2 is spiking but neuron 1 is quiescent, and if $w_{\infty,1} \leq 1$, then neuron 1 will remain quiescent for all time. On the other hand, if $w_{\infty,1} > 1$, then neuron 1 will spike after a finite time interval. Now we can state our two main results.

Theorem 3.8. *For model (1), consider the initial condition $\mathbf{v}_0 = (w_0, 1)$ with $w_0 < 1$. Let $\gamma := \frac{\alpha_1 - g}{\alpha_2 - g}$.*

1. *If $\rho_2 \geq \gamma$ then neuron 1 will remain quiescent for all time.*
2. *If $\rho_2 < \gamma$, then $w_{\infty,1} > 1$ and the first spike in neuron 1 will occur at time t_N where N is given by*

$$N = \left\lceil \frac{\log(w_{\infty,1} - 1) - \log(w_{\infty,1} - w_0)}{\log\left(1 - \frac{g}{\alpha_2}\right)} \right\rceil \tag{2}$$

Proof. By Lemma 3.5, $w_n = w_{\infty,1} + (w_0 - w_{\infty,1})\left(1 - \frac{g}{\alpha_2}\right)^n$ where w_n is the membrane potential of neuron 1 assuming that neuron 2 spikes but neuron 1 does not spike up to time t_n. If $\rho_2 < \gamma$, then there exists an N such that $w_N \geq 1$ but $w_{N-1} < 1$. Then $N = \min\{n : w_n > 1\}$ from which the result follows. □

The next result, which is the main theorem of this section, shows that for the voltage-based integrate-and-fire model, the only stability regimes are the monostable regimes M0, M1, M2 and the bistable regime B. The impossibility of B1, B2 and T is due to the fact that if $\mathcal{Q}_1^c \cap \mathcal{Q}_2$ is a stable mode and neuron 1 fires at least one spike, then neuron 2 will be quiescent for all time, thus ruling out the co-existence of the stable mode $\mathcal{Q}_1^c \cap \mathcal{Q}_2^c$. By similar reasoning, the stable mode $\mathcal{Q}_1^c \cap \mathcal{Q}_2^c$ cannot co-exist with the stable mode $\mathcal{Q}_1 \cap \mathcal{Q}_2^c$ in model (1). Thus, B1, B2 and T are ruled out for the voltage-based integrate-and-fire model. We will show in the next section that the non-instantaneous inhibition time in the current-based integrate-and-fire model does allow for B1, B2 and T.

Theorem 3.9. *Consider model (1) of a reciprocally inhibiting pair of neurons and let $\Gamma_{2,1} = \frac{\rho_2(\alpha_2 - g)}{\alpha_1 - g}$ and $\Gamma_{1,2} = \frac{\rho_1(\alpha_1 - g)}{\alpha_2 - g}$.*

1. *If $\Gamma_{2,1} \geq 1 > \Gamma_{1,2}$, then the system is monostable – type M1, i.e. for all initial conditions, neuron 1 is active for all time while neuron 2 is quiescent for all time (after possibly firing finitely many spikes).*
2. *If $\Gamma_{1,2} \geq 1 > \Gamma_{2,1}$, then the system is monostable – type M2, i.e. for all initial conditions, neuron 2 is active for all time while neuron 1 is quiescent for all time (after possibly firing finitely many spikes).*
3. *If $\Gamma_{2,1} < 1$ and $\Gamma_{1,2} < 1$, then the system is monostable – type M0, i.e. for all initial conditions, both neurons remain actively firing for all time.*
4. *If $\Gamma_{2,1} \geq 1$ and $\Gamma_{1,2} \geq 1$, then the neuron that fires the first spike remains active for all time, while the other neuron remains quiescent for all time. If both neurons fire the first spike together, then whichever neuron fires the second spike remains active for all time, while the other neuron remains quiescent for all time after the first spike. If both neurons fire the first two spikes together, then both neurons fire simultaneously for all time. In other words, the system is bistable – type B.*

Proof. $\Gamma_{2,1} \geq 1 > \Gamma_{1,2}$. By Theorem 3.8, for all initial conditions, neuron 1 will spike after a finite time interval, after which neuron 2 will be quiescent for all time. The second case is similar with roles of 1 and 2 interchanged. In the third case, neither neuron supplies sufficient inhibition to keep the other neuron quiescent, even when firing at its uncoupled frequency. When coupled, and when both neurons are active, the firing frequency of each neuron is lowered and thus the timed-averaged inhibition that it provides the other neuron is also lowered. Thus both neurons remain

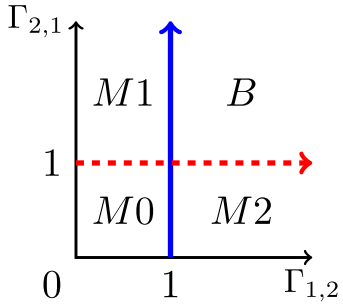

Fig. 2. The values of $\Gamma_{1,2}$ and $\Gamma_{2,1}$ determine the stability regime $M0$, $M1$, $M2$, B of the system. The four stable modes provide a full classification of the voltage-based integrate-and-fire model.

actively firing for all time. In the fourth case, both neurons supply sufficient inhibition to keep the other neuron quiescent, thus whichever neuron fires first will remain active for all time while the other neuron will remain quiescent for all time. □

For a bistable system B, we partition the set of initial conditions into regions where: (i) neuron 1 is active for all time and neuron 2 is quiescent for all time (possibly after an initial transient), and another region where (ii) neuron 2 is active for all time and neuron 1 is quiescent for all time (possibly after an initial transient). Between these two stable regions, there is an unstable region (i.e. one that does not contain an open disk) where both neurons fire simultaneously for all time (Fig. 2).

Proposition 3.10. *Consider model (1) of a reciprocally inhibiting pair of neurons and suppose that* $\Gamma_{2,1} = \frac{\rho_2(\alpha_2-g)}{\alpha_1-g} \geq 1$ *and* $\Gamma_{1,2} = \frac{\rho_1(\alpha_1-g)}{\alpha_2-g} \geq 1$. *Suppose that initially* $(V_1(0), V_2(0)) = (u_1, u_2) \in (-\infty, 1) \times (-\infty, 1)$. *Let* $i, j \in \{1, 2\}$ *with* $i \neq j$. *Then the following holds:*

1. *Suppose that*
$$\frac{\alpha_j - gu_j}{\alpha_j - g} < \frac{\alpha_i - gu_i}{\alpha_i - g}. \tag{3}$$
Then neuron j is active for all time, and neuron i is quiescent for all time.
2. *Suppose that*
$$\frac{\alpha_j - gu_j}{\alpha_j - g} = \frac{\alpha_i - gu_i}{\alpha_i - g}$$
$$\frac{\alpha_j + g\rho_i}{\alpha_j - g} < \frac{\alpha_i + g\rho_j}{\alpha_i - g} \tag{4}$$
Then neuron i and neuron j fire the first spike simultaneously, then neuron j is active for all time, and neuron i is quiescent for all time after the first spike.
3. *Suppose that*
$$\frac{\alpha_j - gu_j}{\alpha_j - g} = \frac{\alpha_i - gu_i}{\alpha_i - g}$$
$$\frac{\alpha_j + g\rho_i}{\alpha_j - g} = \frac{\alpha_i + g\rho_j}{\alpha_i - g} \tag{5}$$
Then neuron i and neuron j remain active for all time and the two neurons always spike simultaneously.

Proof. Since $\Gamma_{2,1} \geq 1$ and $\Gamma_{1,2} \geq 1$, the system is bistable – type *B*. Suppose that $(V_1(0), V_2(0)) = (u_1, u_2)$. The time to first spike in the absence of inhibition for neuron $i \in \{1, 2\}$ is $\sigma_i = -\frac{1}{g} \ln\left(\frac{\alpha_i - g}{\alpha_i - gu_i}\right)$. If neuron i fires before the other neuron j, i.e. $\sigma_i < \sigma_j$, then neuron i remains actively firing for all time and neuron j remains quiescent for all time. The condition in (3) is equivalent to $\sigma_i < \sigma_j$. This proves part (1) of the statement.

Suppose now that $\frac{\alpha_j - gu_j}{\alpha_j - g} = \frac{\alpha_i - gu_i}{\alpha_i - g}$. In that case, both neurons i and j fire the first spike together. After this spike, neuron 1 is reset of $-\rho_2$ and neuron 2 is reset to $-\rho_1$. In this case, we simply apply (3) with $u_1 = -\rho_2$ and $u_2 = -\rho_1$ to determine which neuron fires the next spike. If neuron i fires before neuron j, then i remains active for all time and j remains quiescent for all time. This proves part (2) of the statement.

Finally, suppose that the condition in (5) holds. Then the neurons fire the first and the second spike simultaneously, after which their voltages are reset to $(-\rho_2, -\rho_1)$. Since these are the same initial voltages after the first spike, the two neurons continue to spike simultaneously for all time thereafter. This proves part (3) of the statement. □

Thus, for the voltage-based integrate-and-fire model, we get a full classification of long-term dynamical behaviors and the precise dependence of these dynamics on the system parameters. We will see that the dynamic range of behaviors is enlarged when we move to a more realistic current-based integrate-and-fire model in the next section. Specifically, all seven stability regimes ($M0$, $M1$, $M2$, B, $B1$, $B2$, T) will be shown to exist.

4. Current-based I&F Model

An alternative to the voltage-based integrate-and-fire model is a current-based model where an inhibitory current lasts over a positive time interval. Each neuron is modeled as an integrate-and-fire neuron; the membrane potential of neuron j ($j \in \{1, 2\}$) is governed by the following equation:

$$\frac{dV_j}{dt} = -gV_j + \alpha_j - I_j(t) \text{ , where}$$
$$I_j(t) = \beta_j \sum_i (H(t - \tau_k^i) - H(t - \tau_k^i - h_j))$$
$$V_j(t) = 1 \Rightarrow \{V_j(t^+) = 0\} \tag{6}$$

where $V_j(t)$ is the membrane potential, and $g = 0.05$ is the leak conductance. The model is reduced dimensional, with a nondimensional membrane potential, time in units of ms, and conductance in units of ms^{-1}. A spike is recorded when $V_j(t)$ reaches a threshold value $E_{thresh} = 1$, with $V_j(t)$ being instantaneously reset to the rest potential of 0 following a spike. Details of the reduced dimensional model are given in Tao et al. (2004). An absolute refractory period of $r = 2$ ms is simulated by holding the membrane potential at rest for $r = 2$ ms following a spike. For computational results, simulations were carried out using the explicit Euler method with a time step of 0.0001ms (the small time step is needed for precise resolution of analytically computed bifurcation points).

Each neuron receives a constant excitatory current given by the value α_j. Synaptic inhibition is current-based and modeled through the $I_j(t)$ term. If neuron $k \neq j$ spikes at time τ_k, then $I_j(t)$ is incremented by an amount β_j at time τ_k and decremented by β_j at time $\tau_k + h_j$. We refer to β_1, β_2 as the amplitude of inhibition of neurons 1 and 2 respectively, and we refer to h_1, h_2 as the time course of inhibition of neurons 1 and 2, respectively. H represents the Heaviside step function, $\tau_k^1, \tau_k^2, \tau_k^3, \ldots$ are the spike times of the neuron k.

We considered an alternate model, where the inhibitory current jumps up by a fixed amount β_j as in (6), and the current $I_j(t)$ decays exponentially between jumps.

$$\dot{V}_j = -gV_j - I_j(t) + \alpha_j$$
$$\dot{I}_j = -I_j/\tilde{h}_j + \beta_j \sum_i \delta(t - \tau_k^i) \tag{7}$$

Here $\tilde{h}_j$ represents the current decay time, and δ represents the Dirac delta. We present the analytical results obtained for model

in (6), and will make no further mention of the model in (7), since the results for the two models are quite analogous.

At a steady state, each neuron is either actively spiking for all time or quiescent for all time based on the balance between excitation and inhibition that the neuron receives. If a neuron, say neuron 1, receives enough excitation to overcome the maximum inhibition that the other neuron (neuron 2) delivers, then neuron 1 will continue to spike for all time. The maximum spiking frequency of neuron 2 occurs when neuron 2 receives no inhibition from neuron 1. Reasoning similarly to Section 3, under the assumption that $\alpha_2 > g$ and no inhibition, neuron 2 spikes with period $T_2 = -\ln(1-g/\alpha_2)/g$, or if we impose a post-spike refractory period of $r > 0$, $T_2 = r - \ln(1-g/\alpha_2)/g$. Thus neuron 1 receives an inhibitory current I_1 with period T_2.

We assume, without loss of generality, that neuron 2 spikes at times kT_2, where $k \in \mathbb{Z}$. In order to determine the subthreshold membrane potential of neuron 1 under the periodic inhibitory current from neuron 2, we solve (6) or equivalently:

$$\dot{V} = -gV + \alpha - I(t)$$
$$I(t) = \begin{cases} (n+1)\beta, & kT \le t \le kT + h - nT \\ n\beta, & kT + h - nT \le t < (k+1)T \end{cases} \quad (k \in \mathbb{Z}) \tag{8}$$

where we suppressed the indices labeling the neurons, and $n := \lfloor h/T \rfloor$.

Proposition 4.1. *Consider a neuron whose membrane potential is governed by (8). For all initial conditions $V(0) < 1$, the neuron will continue to spike for all time (after some initial transient) if the following condition is satisfied:*

$$\alpha - g \ge \beta \left[n + \frac{e^{g(h-nT)} - 1}{e^{gT} - 1} \right], \tag{9}$$

where $n = \lfloor \frac{h}{T} \rfloor$.

Proof. We prove the contrapositive. Suppose that neuron 1 is quiescent for all time, i.e. $\limsup_{t\in\mathbb{R}} V(t) < 1$. Let $\widetilde{V}(t)$ denote the steady state membrane potential. From (8), $\widetilde{V}(t)$ is periodic with period T, and for all $k \in \mathbb{Z}$, $\widetilde{V}(t)$ is monotone on $[kT, kT + h - nT]$ and on $[kT + h - nT, (k+1)T]$. Since the inhibitory current on the former interval is $(n+1)\beta$, which is greater than that on the latter interval $n\beta$, it follows that $\widetilde{V}(t)$ is decreasing on the former interval and increasing on the latter interval. Therefore, $\limsup_{t\in\mathbb{R}} V(t) = \limsup_{k\in\mathbb{Z}} V(kT) = \widetilde{V}(kT)$ for all $k \in \mathbb{Z}$. Finding the steady state solution $\widetilde{V}(t)$ is a simple exercise. When we impose the condition $\widetilde{V}(t) < 1$, we get

$$\alpha - g < \beta \left[n + \frac{e^{g(h-nT)} - 1}{e^{gT} - 1} \right],$$

which proves the claim. □

Theorem 4.2. *Consider the model (6) and suppose that the parameters satisfy*

$$\alpha_1 - g \ge \beta_1 \left(\left\lfloor \frac{h_1}{T_2} \right\rfloor + \frac{e^{g(h_1 - \lfloor h_1/T_2 \rfloor T_2)} - 1}{e^{gT_2} - 1} \right), \tag{10}$$

where $T_2 = r - \ln(1-g/\alpha_2)/g$. Then for all initial conditions $V_1(0) \le 1$, $V_2(0) \le 1$, neuron 1 will fire a spike at some finite positive time, and will continue to spike thereafter.

Proof. The proof is immediate from Proposition 4.1 and the observation that neuron 2 has the maximum spiking frequency when it is spiking with period given by T_2. □

In the following analysis, we will refer to (10), with '$\ge$' replaced by '$<$', as the suppression condition for neuron 1, and the analogous statement (with the '1' and '2' indices reversed) as the suppression condition for neuron 2. Thus, we define the *suppression condition for neuron j* (j, $k \in 1, 2$, $j \ne k$) as

$$\alpha_j - g < \beta_j \left(\left\lfloor \frac{h_j}{T_k} \right\rfloor + \frac{e^{g(h_j - \lfloor h_j/T_k \rfloor T_k)} - 1}{e^{gT_k} - 1} \right), \tag{11}$$

where $T_k = r - \ln(1-g/\alpha_k)/g$. If the suppression condition for neuron j is satisfied, then, under the assumption that $I_k(t)=0$, neuron j is guaranteed to remain quiescent for all time (after a possible initial transient). We will use the analytically derived suppression condition to plot bifurcation curves and stability diagrams in parameter space for the two-neuron system, and we will verify the analytically derived results with simulations. We begin with the simplest case, where all parameters are symmetric between the two neurons, then proceed to the general, asymmetric case. Finally, we will examine the behavior of the system in the case that the excitatory currents to the two cells are allowed to be noisy.

4.1. Symmetric case

In the symmetric case, where $\alpha_1 = \alpha_2 = \alpha$, $\beta_1 = \beta_2 = \beta$, and $h_1 = h_2 = h$, the system has only 3 three bifurcation parameters (α, β, h). Since the *suppression condition for neuron 1* is identical to the *suppression condition for neuron 2*, both conditions must be simultaneously violated or simultaneously satisfied, and we therefore expect that the system will either be monostable with both neurons spiking for all time or bistable with one neuron active and the other silent (with the identity of the active and silent neurons determined by the initial conditions). We can then plot the surface in α, β, h space obtained by replacing the inequality in the *suppression condition for neuron j* ((11)) by equality; this surface separates the monostable from the bistable regime (Fig. 3A, *left*). In the right panel of Fig. 3A, we show the cross-section of this surface given by fixing $\alpha = 0.5$. In Fig. 3B, we fix $\alpha = 0.5$ and $h = 5$, and we show computationally derived plots of the spiking activity of neurons 1 and 2 as β is increased through the bifurcation value of $\beta_c = 0.037495$. For $\beta < \beta_c$, we see that the system is indeed monostable, while for $\beta > \beta_c$, we find that the system is bistable (in the plots, neuron 1 is quiescent with neuron 2 active, but since all parameters are symmetric, a reversal of the initial conditions will yield the reciprocal behavior). Interestingly, we see that as β approaches β_c from the monostable side, the spiking behavior of the two neurons (while remaining monostable) resembles the bistable regime more and more.

4.2. General case

In the general case, where asymmetry is permitted in all system parameters, the system contains six bifurcation parameters: α_1, α_2, β_1, β_2, h_1, h_2. Based on the suppression condition derived earlier, we expect that, depending on the values of the bifurcation parameters, our two-neuron system may fall into one of four distinct dynamical regimes: (1) *suppression conditions for neurons 1 and 2* are both violated; (2) *suppression condition for neuron 1* is violated while *suppression condition for neuron 2* is satisfied; (3) *suppression condition for neuron 1* is satisfied while *suppression condition for neuron 2* is violated; (4) *suppression conditions for neurons 1 and 2* are both satisfied. We expect that in regime (1), both neurons will spike for all time (monostable; M0). We expect that in regime (2), neuron 1 will spike for all time while neuron 2 will be silent (monostable; M1), while in regime (3) the opposite will occur (monostable; M2). In regime (4), however, we expect that the system will be bistable (B) – one neuron will spike for all time while the other will be quiescent, with the identity of the active and passive cells determined by the initial conditions. Fig. 4A summarizes these four dynamical regimes.

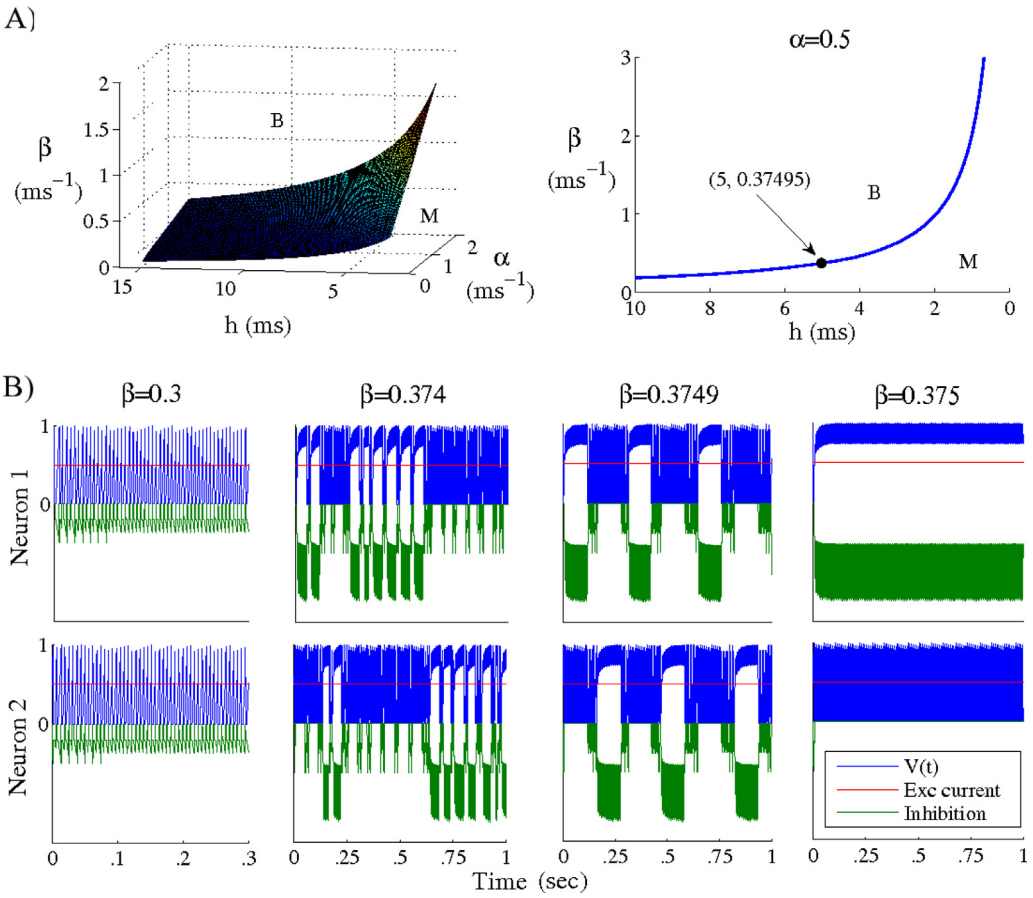

Fig. 3. Stability diagrams and spiking activity in the symmetric case: $\alpha_1 = \alpha_2 = \alpha$, $\beta_1 = \beta_2 = \beta$, $h_1 = h_2 = h$ *A)* The left panel shows the analytically derived surface in parameter space separating the monostable from the bistable regimes, while the right panel shows the cross section obtained by fixing $\alpha = 0.5$. *B)* We fix $\alpha = 0.5$ and $h = 5$ and we plot the spiking activity of the two neurons as β is increased through the bifurcation value $\beta_c = 0.37495$. The initial conditions for all β values are given by $V_1(0) = 0.1$, $V_2(0) = 0.9$.

The *suppression condition for neuron j* (11) allows us to plot stability diagrams for the system. We can fix four of the system parameters and derive a suppression curve for neuron j ($j \in \{1, 2\}$) in the plane defined by the remaining two parameters by replacing the inequality in (11) by equality. The suppression curve for neuron j partitions the parameter plane into two regions: in one region, neuron j spikes repetitively for all time, while in the other region, neuron j is quiescent for all time (after a possible initial transient). If we simultaneously plot the suppression curves for neurons 1 and 2, we obtain a stability diagram for the system; the two suppression curves intersect at a bifurcation point of co-dimension 2 and partition the parameter plane into the four distinct stability regions {M0, M1, M2, B} described above.

4.2.0.1. Synaptic Inhibition. In Fig. 4B (*top row*) we fix α_1, α_2, h_1, h_2 at various values and plot stability diagrams in the β_1, β_2 plane, while in Fig. 4B (*bottom row*) we fix α_1, α_2, β_1, β_2 at various values and plot stability diagrams in the h_1, h_2 plane. As would be expected from the $I_k(t) = 0$ assumption in the derivation of (11), the suppression curves of neurons 1 and 2 are parallel to the y-axis and x-axis, respectively. This indicates that synaptic inhibition exerts *independent control* over the behavior of the two neurons: whether neuron j spikes repetitively for all time or remains quiescent for all time depends on the parameters β_j, h_j with no dependence on β_k, h_k ($k \neq j$). In other words, with α_j, α_k fixed, the behavior of neuron j depends only on the parameters governing synaptic inhibition to neuron j and not on the parameters governing the inhibitory current to neuron k.

In accordance with this *independent control*, Fig. 4B shows that if the fixed value of h_2 (*top row*) or β_2 (*bottom row*) is altered, then the suppression curve for neuron 2 undergoes a vertical shift while the suppression curve for neuron 1 remains unchanged. On the other hand, altering the fixed value of α_2 (*top and bottom rows*) shifts the suppression curves of *both* neurons, suggesting that the excitatory current does *not* exert independent control over the behavior of the two neurons (see next section). The accuracy of the analytically derived stability diagrams is verified computationally in Fig. 5. Fig. 5A shows one of the stability diagrams from Fig. 4 as well as showing a close-up of the bifurcation point. In Fig. 5B, we fix h_1, h_2, α_1, α_2 at the values from Fig. 5A, and we plot the spiking activity of neurons 1 and 2 when β_1, β_2 assume values in each of the four stability regions {M0, M1, M2, B} extremely close to the bifurcation point; spiking activity is shown for two initial conditions (IC1: $V_1(0) = 0.1, V_2(0) = 0.9$; IC2: $V_1(0) = 0.9, V_2(0) = 0.1$). In the M0 regime, we see that both initial conditions lead to the same behavior (both neurons spiking concurrently for all time). In the M1 regime, we see that for both initial conditions, the system converges to neuron 1 spiking for all time with neuron 2 silent, while the reciprocal behavior occurs in the M2 regime. In the B regime, we see bistability – IC1 leads to neuron 2 spiking for all time with neuron 1 silent, while IC2 leads to neuron 1 spiking for all time with neuron 2 silent.

Excitatory Current. As alluded to in the previous paragraph, the excitatory current does not appear to exert independent control over the behavior of the two neurons, in the sense that varying α_j can

A)

Stability Regime	Description
M0	Monostable; both neurons fire simultaneously
M1	Monostable; neuron 1 fires with neuron 2 quiet
M2	Monostable; neuron 2 fires with neuron 1 quiet
B	Bistable; one neuron fires with the other quiet

B)

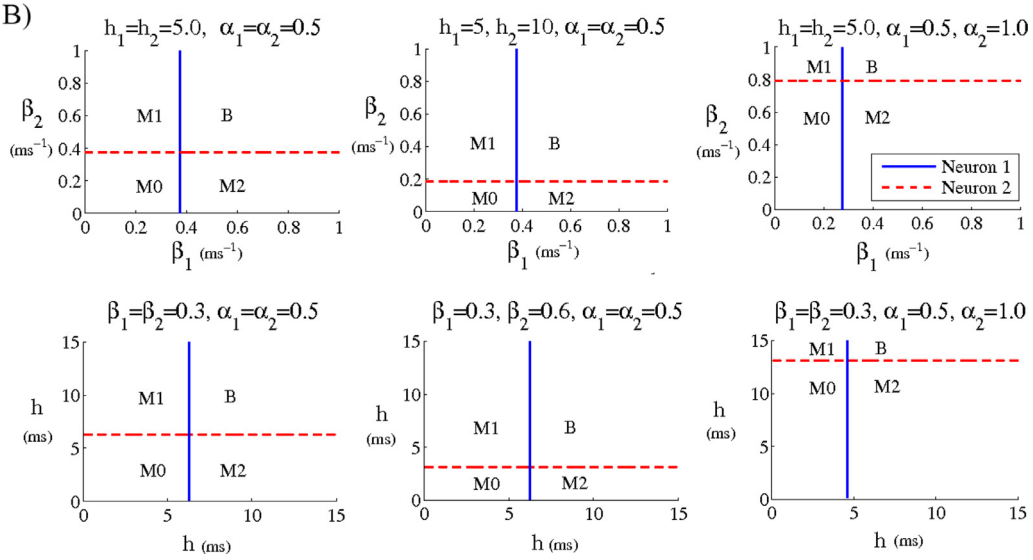

Fig. 4. *(A)* Possible stability regimes based on the analytic suppression condition. *(B)* Stability diagrams for synaptic inhibition parameters. In the top row, we fix α_1, α_2, h_1, h_2 at various values and plot the *suppression condition for neuron 1* and the *suppression condition for neuron 2*, with the inequality in (11) replaced by equality, in the β_1, β_2 plane. In the bottom row, we fix α_1, α_2, β_1, β_2 at various values and plot the suppression conditions in the h_1, h_2 plane. We expect that the suppression curves for neurons 1 and 2 obtained partition the plane into distinct stability regimes.

affect the repetitive spiking vs. quiescence behavior of *both* neurons (rather than just neuron j). In Fig. 6, we explicitly show this lack of independent control by fixing β_1, β_2, h_1, h_2 at various values and plotting stability diagrams for the system in the α_1, α_2 plane. We only consider the case where $\alpha_1, \alpha_2 > g = 0.05$ (since $\alpha_j = g$ is the critical level of excitation required to induce spiking in neuron j, the cases where $\alpha_j \leq g$ is satisifed for one or both neurons lead to obvious behavior). The suppression curves for the two neurons in Fig. 6 are not parallel to the x-axis or y-axis, and it is apparent that it is possible to alter the behavior of both neurons by varying *either* α_1 *or* α_2 alone.

If the synaptic inhibition parameters β_1, β_2, h_1, h_2 are sufficiently small, then neither neuron is capable of silencing the other, regardless of the values of α_1 or α_2, and the entire segment α_1, $\alpha_2 > g$ of the α_1, α_2 plane will correspond to a single stability regime: M0. The reason this scenario can occur for nonzero values of the synaptic inhibition parameters is because the absolute refractory period of $r = 2$ ms within our model imposes an upper bound on the spike rate of the two neurons, limiting the amount of inhibition that one neuron can deliver to the other for fixed β_1, β_2, h_1, h_2. If we increase β_j or h_j slightly while leaving the synaptic inhibition parameters for the other neuron (β_k, h_k) small, a suppression curve for neuron j materializes in the α_1, $\alpha_2 > g$ segment of the plane, partitioning the α_1, $\alpha_2 > g$ segment of the plane into two stability regions: M0, Mj. If we then increase β_k or h_k slightly, a suppression curve for neuron k materializes in the α_1, $\alpha_2 > g$ segment of the plane as well; however, the suppression curves for neurons j and k do not intersect, and the α_1, $\alpha_2 > g$ segment of the plane is partitioned into three stability regions: M0, M1, M2 (Fig. 6, *top left*).

This lack of intersection is possible because α_j controls *both* the amount of inhibition delivered by neuron j to neuron k *as well as* the ability of neuron j to surmount the inhibition incoming from neuron k. In the inhibitory regime where a lack of intersection occurs, the inhibitory parameters are such that neuron j can silence neuron k only if α_j is high *and* α_k is low – neuron k will be silenced only if α_j is high enough for neuron j to deliver strong inhibition and α_k is low enough to prevent neuron k from overcoming this inhibition. Likewise, α_k must be high with α_j low in order for neuron k to silence neuron j, and there does not exist a pair of values α_j, α_k which allows both neuron j to potentially quiet neuron k and neuron k to potentially quiet neuron j. Thus, no pair of values α_1, α_2 yields the bistable behavior B.

If we further increase the synaptic inhibition parameters for neuron 1 or 2 (or both), the suppression curve for neuron 1 will exhibit slower growth or the suppression curve for neuron 2 will exhibit steeper growth in the α_1, $\alpha_2 > g$ segment of the plane (or both), leading to an intersection (a bifurcation point of co-dimension 2) and creating a fourth stability region: B. Within such an inhibitory regime, the inhibitory parameters are such that there exist a pair of values α_1, α_2 that allow each neuron to potentially silence the other. This is shown in Fig. 6, in which we plot the stability diagram within an inhibitory regime where an intersection occurs (*top right*) and we show how the stability diagram changes when either β_2 (*bottom left*) or h_2 (*bottom right*) is increased in isolation.

Other Stability Regimes. Thus, similar to the voltage-based integrate-and-fire model, we find that in the current-based integrate-and-fire model there exist the basic stability regions {M0, M1, M2, B} of parameter space and that these regions can be found analytically. In the voltage-based integrate-and-fire model, a comprehensive analysis of model behavior was possible, and we were able to show with mathematical rigor that these four

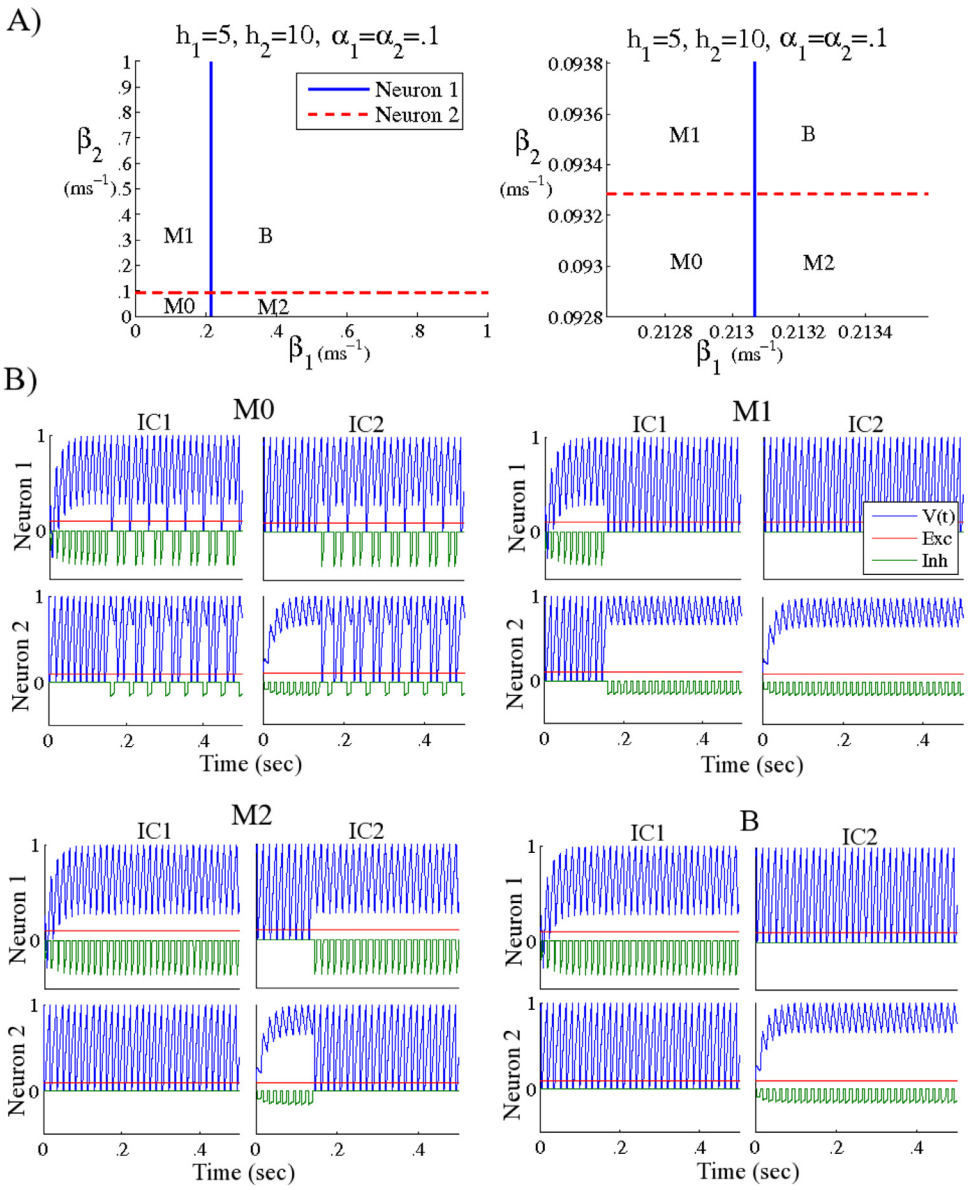

Fig. 5. *(A)* Stability diagram of the system in the β_1, β_2 plane with a zoom-in of the bifurcation point in the right panel. *(B)* Spiking activity of neurons 1 and 2 is shown when β_1, β_2 assume values in the M0 region ($\beta_1 = 0.2130, \beta_2 = 0.0932$), M1 region ($\beta_1 = 0.2130, \beta_2 = 0.0934$), M2 region ($\beta_1 = 0.2132, \beta_2 = 0.0932$), and B region ($\beta_1 = 0.2132, \beta_2 = 0.0934$). Spiking is shown for two initial conditions – IC1: $V_1(0) = 0.1, V_2(0) = 0.9$; IC2: $V_1(0) = 0.9, V_2(0) = 0.1$.

stability regions of parameter space exhaust all possible behaviors of the system. In the current-based model, however, an exhaustive mathematical analysis of model behavior is more difficult, but through computational investigations we now show that additional stability regions beyond the basic {M0, M1, M2, B} regions can exist within parameter space, and that the existence of these additional stability regions is due to the temporal dynamics of synaptic input (in the voltage-based model, synaptic input is instantaneous and has no dynamics).

In the derivation of the *suppression condition for neuron j* (11), we assumed $I_k(t) = 0$ (i.e., that neuron k receives no inhibition from neuron j), and we provided computational evidence in the Synaptic Inhibition section that the stability diagrams obtained under this assumption are accurate. However, it is reasonable to expect that, under certain conditions, nonzero $I_k(t)$ may have an impact on the dynamical behavior of the system. We can then ask: under what conditions might nonzero $I_k(t)$ lead to a deviation from the dynamical steady-state behavior deduced from the stability diagrams given by (11)?

Through computational investigations, we find that, in some parameter regimes, there exist additional bistable regions near co-dimension 2 bifurcation points in the stability diagrams other than the {M0, M1, M2, B} regions deduced from (11). Fig. 7A shows a stability diagram in the β_1, β_2 plane in which an additional bistable state exists near the co-dimension 2 bifurcation point. Fig. 7B shows spiking activity of the two neurons for two initial conditions (IC1: $V_1(0) = 0.1, V_2(0) = 0.9$; IC2: $V_1(0) = 0.9, V_2(0) = 0.1$) for β_1, β_2 values that place the system in the M1 region near the bifurcation point or far from the bifurcation point. Far from the bifurcation point, we see that the system exhibits the monostable behavior M1, while near the bifurcation point the system actually exhibits bistable behavior not previously encountered (which we will denote B1). The bistable state B1 is given by both neurons spiking simultaneously for all time (one stable state) or neuron 1 spiking for all time with neuron 2 quiet for all time (the other sta-

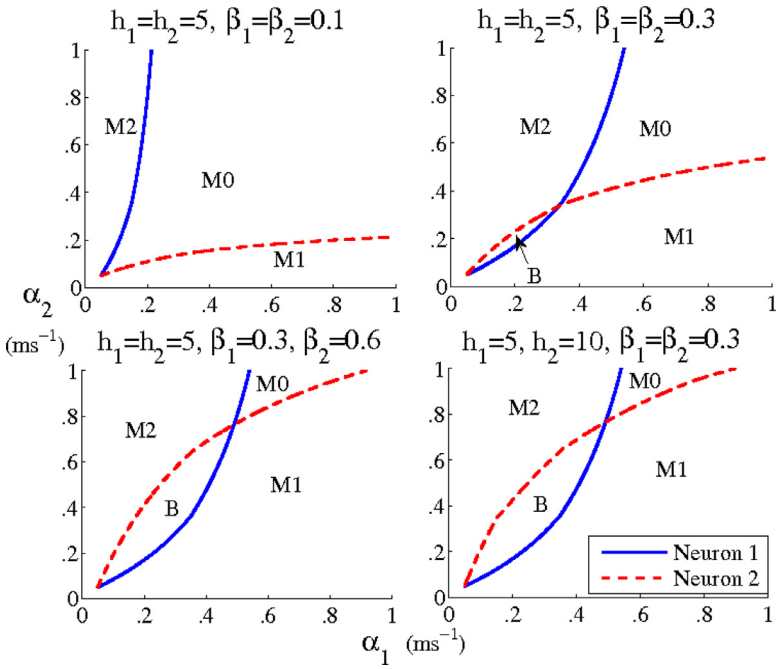

Fig. 6. Stability diagrams of the system in the α_1, α_2 plane for $\alpha_1, \alpha_2 > g = 0.05$. For weak mutual inhibition (*top left*, the suppression curves for the two neurons do not intersect, and three monostable stability regions exist: M0, M1, M2. For sufficiently strong synaptic inhibition (*other panels*), the suppression curves intersect and create a fourth bistable stability region: B.

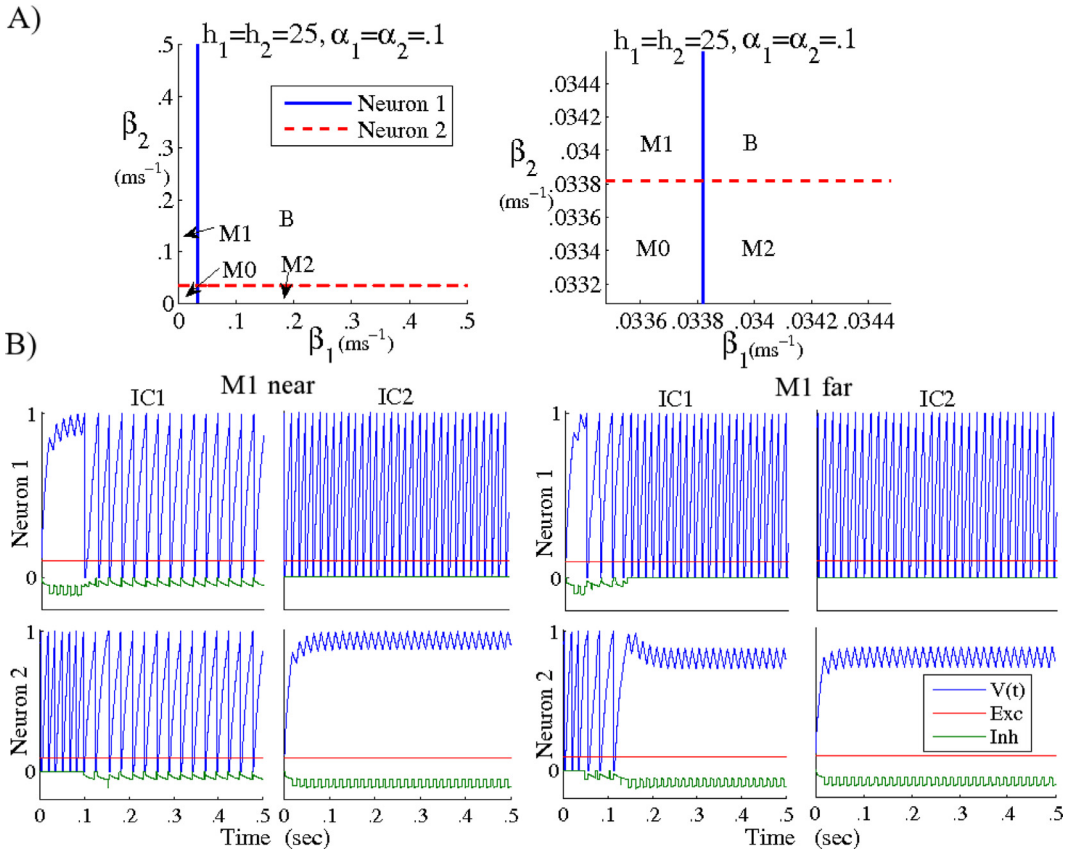

Fig. 7. A regime in which stability regions other than {M0, M1, M2, B} exist in the β_1, β_2 plane. *A)* A stability diagram in the β_1, β_2 plane in which additional stability regions exist (*left*), with a zoom-in of the bifurcation point *right. B)* Spiking plots of neurons 1 and 2 are shown for β_1, β_2 in the M1 region near the bifurcation point ($\beta_1 = 0.0337, \beta_2 = 0.0339$) and far from the bifurcation point ($\beta_1 = 0.0310, \beta_2 = 0.0380$). In the M1 region near the bifurcation point, the system actually exhibits bistability (B1). Spiking is shown for two initial conditions – IC1: $V_1(0) = 0.1, V_2(0) = 0.9$; IC2: $V_1(0) = 0.9, V_2(0) = 0.1$.

ble state). This implies that there can also exist bistable behavior denoted by B2 (for β_1, β_2 in the M2 region near the bifurcation point) in which either both neurons spike concurrently or neuron 2 spikes with neuron 1 silent.

Under what conditions do we expect the B1 and B2 stability regions to exist? Suppose our parameter values place the system in the M1 stability region. If the initial conditions are such that neuron 1 fires before neuron 2, then (since neuron 1 is capable of silencing neuron 2 within the M1 region), neuron 2 will never fire and the system will approach the stable state given by neuron 1 firing and neuron 2 quiescent. If the initial conditions are such that neuron 2 begins firing before neuron 1, it is guaranteed that neuron 1 will eventually fire (since neuron 2 is not capable of silencing neuron 1 in the M1 stability region). In the following argument, suppose the initial conditions result in neuron 2 firing before neuron 1. We can expect distinct qualitative behavior in the case $h_1 < T_2$ versus the case $h_1 > T_2$, where h_1 is the time course of synaptic inhibition from neuron 2 to neuron 1 and T_2 is the interspike interval of neuron 2 when $I_2(t) = 0$.

First, suppose $h_1 < T_2$ (i.e., suppose the time course of synaptic inhibition from neuron 2 to neuron 1 is smaller than the interspike interval of neuron 2). In this case, neuron 2 delivers an inhibitory current to neuron 1 $I_1(t)$ which is guaranteed to go to zero prior to the next spike of neuron 2; $I_1(t)$ jumps when neuron 2 spikes, but, since $h_1 < T_2$, $I_1(t)$ jumps back down to zero prior to the next spike of neuron 2. When neuron 1 spikes (and it is guaranteed that it will, since we are in the M1 stability region), it is likely to spike at a time t_s such that $I_1(t_s) = 0$. Since neuron 1 is capable of silencing neuron 2, neuron 2 will likely be prevented from spiking prior to the next spike of neuron 1, and since neuron 1 is not receiving any inhibition ($I_1(t) = 0$), the next spike of neuron 1 will occur at time $t_s + T_1$. With the $I_1(t) = 0$ assumption in the derivation of the *suppression condition for neuron 2* satisfied, neuron 1 will spike with an interspike interval of T_1 ms, and the *suppression condition for neuron 2* then guarantees that neuron 2 will be silenced for all time. Thus, for $h_1 < T_2$, we expect that no choice of parameters will yield the B1 stability regime (all initial conditions will lead to the stable state given by neuron 1 spiking forever with neuron 2 silent, and the system will exhibit M1 stability behavior).

Next, suppose $h_1 > T_2$ (i.e., suppose the time course of synaptic inhibition from neuron 2 to neuron 1 is larger than the interspike interval of neuron 2). In this case, neuron 2 delivers an inhibitory current to neuron 1 which may never go to zero; $I_1(t)$ jumps when neuron 2 spikes, but, since $h_1 > T_2$, it is guaranteed that $I_1(t) > 0$ when neuron 1 produces its first spike (since we are in the M1 region, neuron 2 is unable to silence neuron 1, and hence it is guaranteed that neuron 1 will eventually produce a spike). Thus, if neuron 1 spikes at time t_s, we have that $I_1(t_s) > 0$, implying that the next spike of neuron 1 will occur at a time $t_s + T_1 + \epsilon$, where $\epsilon > 0$ is the delay in the interspike interval of neuron 1 induced by the nonzero inhibitory current $I_1(t)$. If ϵ is large enough (i.e., if the parameter β_1 governing the amplitude of synaptic inhibition from neuron 2 to neuron 1 is large, or close to the neuron 1 suppression curve in the M1 segment of the β_1, β_2 plane), and if the parameter β_2 governing the amplitude of synaptic inhibition from neuron 1 to neuron 2 is small enough (i.e., close to the neuron 2 suppression curve in the M1 segment of the β_1, β_2 plane), then neuron 1 may be unable to deliver the inhibition necessary to quiet neuron 2. In this scenario, neuron 2 will spike again, maintaining a minimum $T_1 + \epsilon$ interspike interval of neuron 1, and so neuron 2 will be able to perpetually spike. Since we are in the M1 stability region, neuron 2 cannot silence neuron 1, and so neuron 1 will also spike for all time. This scenario therefore leads to the B1 stability regime: if neuron 1 spikes first, the system converges to the stable state given by neuron 1 spiking perpetually with neuron 2 quiescent, while if neuron 2 spikes first, then the system converges to the stable state given by both neurons spiking simultaneously for all time.

This argument therefore suggests that for $h_j < T_k$, the Bj stability regime will not exist, while for $h_j > T_k$, a Bj stability region will exist near the co-dimension 2 bifurcation point in the Mj segment of the β_1, β_2 plane. The existence of the B1 and B2 stability regimes is further suggestive of the possible existence of another stability regime - a tristable regime (which we denote by T), in which all three possible stable modes coexist: neurons 1 and 2 both spike repetitively for all time, neuron 1 spikes for all time with neuron 2 quiescent, or neuron 2 spikes for all time with neuron 1 quiescent. If a T stability region exists, it must exist within the B segment of the β_1, β_2 plane, since the latter two behaviors can occur *only if* both the *suppression condition for neuron 1* as well as the *suppression condition for neuron 2* are simultaneously satisfied.

Under what conditions might there exist a portion of parameter space within the B region that actually corresponds to a T stability regime? In a T stability regime, it must be the case that if the initial condition for one of the two neurons is considerably closer to spike threshold than the initial condition for the other neuron, then the closer neuron will suppress the distant neuron for all time – this requirement is met by the simultaneous satisfaction of the suppression conditions for both neurons (i.e., by remaining within the B segment of the parameter plane). However, it must also be the case that if the initial conditions for the two neurons are sufficiently close to each other (i.e., if the initial conditions are within some $\epsilon > 0$ neighborhood of each other), then neither neuron will be able to suppress the other, and both neurons will spike simultaneously for all time. For such a scenario to be possible, we must have *both* $h_1 > T_2$ *and* $h_2 > T_1$, for the reasons elaborated above in the argument for the existence the B1 or B2 stability regimes. If both these conditions hold, and if the parameters β_1 and β_2 governing the amplitudes of synaptic inhibition are small, or close to the neuron 1 and 2 suppression curves, respectively, in the B segment of the β_1, β_2 plane, then, if the initial conditions for neurons 1 and 2 are within a sufficiently small neighborhood of each other, both neurons will initially be able to spike, and inhibition from neuron 1 to neuron 2 will prevent neuron 2 from silencing neuron 1, while inhibition from neuron 2 to neuron 1 will prevent neuron 1 from silencing neuron 2. Thus, both neurons will be active for all time. This argument suggests that if $h_1 > T_2$ *and* $h_2 > T_1$ (i.e., if *both* B1 and B2 stability regimes exist), then a T region will exist within the B segment of the β_1, β_2 plane near the intersection of the neuron 1 and neuron 2 suppression curves. However, this argument also suggests that a T region will *not* exist if neither, or only one, of the B1 and B2 regions exist.

We demonstrate this in Fig. 8, in which we plot stability diagrams in the β_1, β_2 plane derived from (11), but with the boundaries of the {B1, B2, T} regions approximated through computational investigations. We plot stability diagrams in the cases that h_1 is slightly smaller or slightly larger than T_2 and h_2 is slightly smaller or slightly larger than T_1. The stability diagrams suggest that the B1 stability region exists near the intersection of the suppression curves in the M1 region only if $h_1 > T_2$, the B2 stability region exists near the intersection of the suppression curves in the M2 region only if $h_2 > T_1$, and T stability region exists near the intersection of the suppression curves in the B region only if both $h_1 > T_2$ and $h_2 > T_1$. We note that when the B1, B2, or T stability regions exist, they are quite small, requiring sensitive fine-tuning of parameters to place the system in one of these regimes. It is therefore possible that B1, B2, or T stability behavior does not play a significant role in real neuronal systems (or perhaps in the case of two mutually inhibitory *networks* of neurons, these regions are larger); however, it is important to note that such behavior exists. The full set of possible stability behaviors of the system in various parameter regimes is summarized in Table 1.

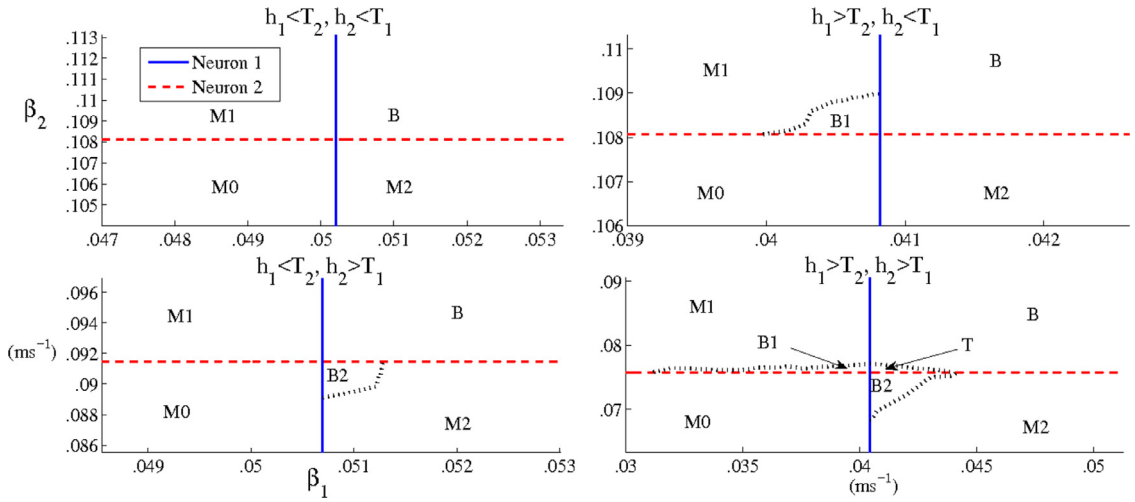

Fig. 8. Stability diagrams of the system in the β_1, β_2 plane. The β_1, β_2 plane is partitioned into stability regions by the suppression curves for neurons 1 and 2 derived analytically from (11). However, (11) cannot provide information about the stability regimes B1, B2, T that may exist near the co-dimension 2 bifurcation point. The boundaries of the {B1, B2, T} stability regions are determined computationally and demarcated by dotted curves. The B1 stability region exists if $h_1 > T_2$, the B2 stability region exists if $h_2 > T_1$, and the T stability region exists if $h_1 > T_2$ and $h_2 > T_1$. In all plots, we fix $\alpha_1 = 0.1, \alpha_2 = 0.15$, which yields $T_1 = 10.1, T_2 = 15.9$. *Top left:* $h_1 = 10, h_2 = 15$. *Top right:* $h_1 = 13, h_2 = 15$. *Bottom left:* $h_1 = 10, h_2 = 18$. *Bottom right:* $h_1 = 13, h_2 = 18$.

Table 1
Summary of stability regimes that exist in the two-neuron system in the cases $\eta_1 < 1$, $\eta_2 > 1$ (*top left*), $\eta_1 > 1$, $\eta_2 > 1$ (*top right*), $\eta_1 < 1$, $\eta_2 < 1$ (*bottom left*), and $\eta_1 > 1$, $\eta_2 < 1$ (*bottom right*). We define $\eta_1 = h_1/T_2$ and $\eta_2 = h_2/T_1$, where h_j is the time course of synaptic inhibition to neuron j and T_j is interspike interval of neuron j in the case that neuron j receives no inhibition.

	$\eta_1 < 1$, $\eta_2 > 1$		$\eta_1 > 1$, $\eta_2 > 1$
M0	Monostable; both neurons fire simultaneously	M0	Monostable; both neurons fire simultaneously
M1	Monostable; neuron 1 fires with neuron 2 quiet	M1	Monostable; neuron 1 fires with neuron 2 quiet
M2	Monostable; neuron 2 fires with neuron 1 quiet	B1	Bistable; either only neuron 1 fires or both neurons fire
B2	Bistable; either only neuron 2 fires or both neurons fire	B2	Bistable; either only neuron 2 fires or both neurons fire
B	Bistable; one neuron fires with the other quiet	B	Bistable; one neuron fires with the other quiet
		T	Tristable; one neuron fires with the other quiet, or both neurons fire
	$\eta_1 < 1$, $\eta_2 < 1$		$\eta_1 > 1$, $\eta_2 < 1$
M0	Monostable; both neurons fire simultaneously	M0	Monostable; both neurons fire simultaneously
M1	Monostable; neuron 1 fires with neuron 2 quiet	M1	Monostable; neuron 1 fires with neuron 2 quiet
M2	Monostable; neuron 2 fires with neuron 1 quiet	B1	Bistable; either only neuron 1 fires or both neurons fire
B	Bistable; one neuron fires with the other quiet	M2	Monostable; neuron 2 fires with neuron 1 quiet
		B	Bistable; one neuron fires with the other quiet

4.3. Stochastic case

In the above, we analyzed the dynamics of the deterministic system given by a pair of mutually inhibitory neurons, each of which receives a constant excitatory driving current. This analysis has implications for the more physiologically meaningful case of mutually inhibitory neurons being driven by noisy excitatory currents. In the case of noisy excitatory currents, we expect distinct dynamical behaviors depending on the stability behavior of the corresponding determinstic system (i.e., the system where noisy excitatory currents are replaced by constant currents, with the value of the constant current given by the mean of noisy excitatory currents). If the corresponding determinstic system is within the M0 regime, we expect both neurons within the noisy system to spike concurrently with little correlation between the firing of the two neurons. If the corresponding determinstic system is within the Mj regime, in the noisy system we expect neuron j to spike without any long pauses between spikes (i.e., with an interspike interval that is approximately constant), while the other neuron exhibits random bouts of spiking activity interrupted by epochs of quiescence. If the corresponding deterministic system is within the B regime, we expect the two neurons to exhibit clear-cut alternating bouts of spiking activity, with random bout times for each neuron.

In order to assess the dynamics of a noisy system, we replace the constant excitatory currents in our model by noisy currents and computationally investigate the spiking behavior of the two neurons. We construct our noisy excitatory currents as follows. The excitatory current $\alpha_j(t)$ jumps by a constant value a_j at a Poisson rate of λ_j (this models excitatory spikes from outside the two-cell system), and decays at a constant rate of $b_j = 1/3$ ms^{-1}. Standard values of the rate and amplitude parameters are given by $\lambda_j^* = 1\text{ms}^{-1}$ and $a_j^* = 0.075$ ms^{-1}. All nonstandard excitatory currents are described in terms of these reference values. We refer to $X_j = a_j\lambda_j$ as the *strength of the excitatory current to neuron j* and we refer to $Y_j = \frac{a_j}{\lambda_j}$ as the *noisiness of the excitatory current to neuron j*. To change the strength of the excitatory current to neuron j by a factor c (without varying the noisiness), we set the rate parameter to $\lambda_j = \sqrt{c}\lambda^*$ and we set the amplitude parameter to $a_j = \sqrt{c}a^*$. To vary the noisiness of the excitatory current to neuron j by a factor d (without changing the strength), we set the rate parameter to $\lambda_j = \frac{\lambda^*}{\sqrt{d}}$ and we set the amplitude parameter to $a_j = \sqrt{d}a^*$. We denote the strength and noisiness of the standard excitatory current by $X^* = \lambda^* a^*$ and $Y^* = \frac{a^*}{\lambda^*}$. Fig. 9 depicts the effects of varying X and Y on the excitatory current.

In order to quantify whether simultaneous spiking or alternating activity bouts are occurring in the noisy system, we devise a measure of the correlation between the spiking activity of the two

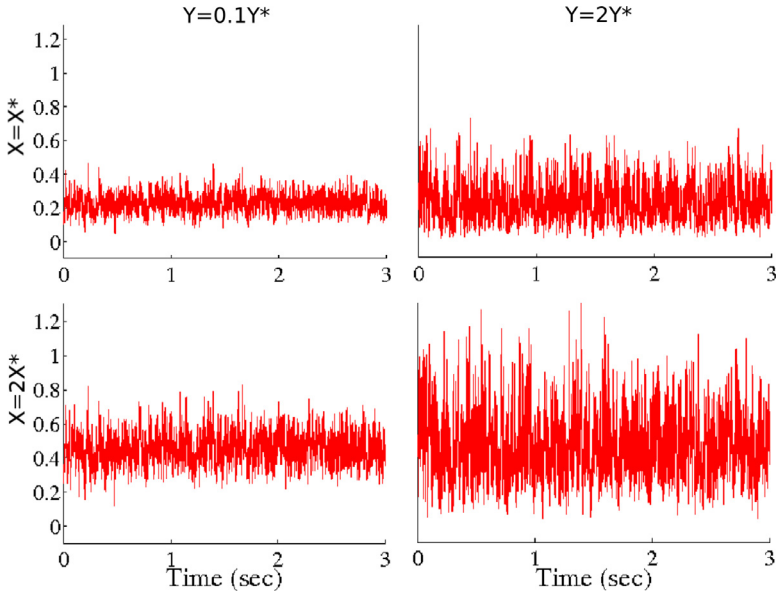

Fig. 9. Effect of varying the strength (X) versus the noisiness (Y) of the noisy excitatory current. One realization of the noisy excitatory current is shown for different combinations of strength (rows) and noisiness (columns).

neurons that we term the *bout index* (BI) of the system. To compute the BI of the system within a particular parameter regime, we obtain 10,000 interspike intervals of neurons 1 and 2, only counting interspike intervals in which the other neuron did not produce a spike; we compute the average interspike intervals ISI_1 and ISI_2 of the two neurons and set $ISI = \min\{ISI_1, ISI_2\}$. We then simulate a 50 second trial of the system, and we parse the trial into successive time windows of length ISI. Within each window, we assign neuron j a 1 if neuron j spiked within the window and a 0 if neuron j did not spike within the window, obtaining a sequence of 0s and 1s for neuron 1 and neuron 2. The BI of the system ($\text{BI} \in [-1, 1]$) is then computed as the correlation between the sequences of 0s and 1s for neurons 1 and 2. If alternating activity bouts are occurring, the BI of the system approaches -1, while if both neurons are spiking concurrently (with little correlation), the BI approaches 0. We experimented with various schemes for defining the *bout index*, and we found the scheme presented in this paragraph to be the best measure of the bout behavior of the system.

In Fig. 10, we fix the inhibitory parameters of the system to obtain the stability diagram (of the corresponding deterministic system) in the α_1, α_2 plane shown in Fig. 10C. In Fig. 10A, we plot spiking activity of the two neurons in the noisy system with the strength of the excitatory currents given by $X_1 = X_2 = 2X^*$ (left), $X_1 = X_2 = 2.5X^*$ (middle), $X_1 = X_2 = 3X^*$ (right), and the noisiness of the excitatory currents fixed at $Y_1 = Y_2 = 0.01Y^*$. In the left panel of Fig. 10A, the mean of the excitatory currents is within the B region, and the system exhibits clear-cut alternating bouts of activity with a *bout index* given by BI=-0.99. In the middle panel of Fig. 10A, the mean of the excitatory currents is near the co-dimension 2 bifurcation point in the α_1, α_2 plane, and the system exhibits some bout behavior intermingled with concurrent spiking and has BI=-0.49. In the right panel of Fig. 10A, the mean of the excitatory currents is within the M0 region, and the two neurons exhibit concurrent, uncorrelated spiking with BI=−0.03. In Fig. 10B, the means of the excitatory currents are within the M2 region ($X_1 = 2.5X^*$, $X_2 = 2.8X^*$; $Y_1 = Y_2 = 0.01Y^*$), with neuron 2 firing continuously and neuron 1 exhibiting bursts of activity interspersed with epochs of silence. In this case, the system has BI=−0.2; this partial correlation between the activity of the two cells occurs because when neuron 2 fires, it is capable of suppressing neuron 1 for a considerable period of time (BI=−1), while when neuron 1 happens to fire, it is incapable of quieting neuron 2, and hence both neurons will fire simultaneously (BI=0). The overall BI of the system is essentially a weighted average of BI=−1 and BI=0, with the weights determined by the relative amounts of time that the system spends in the first or second scenario.

In Fig. 11 (*left*), we fix the inhibitory parameters as in Fig. 10 and we plot the BI of the system as a function of the strength of the noisy excitatory currents to the two neurons ($X = X_1 = X_2$) for several different noisiness values ($Y = Y_1 = Y_2$). As the strength of the excitatory currents is increased from $X = 0.5$ to $X = 5$, the BI of the system rises from -1 to 0 as the system traverses the diagonal in the stability diagram (of the corresponding deterministic system) shown in Fig. 10C (at $X =\sim 2.5X^*$, the corresponding deterministic system is near the co-dimension 2 bifurcation and we have BI=~ -0.5). This occurs because the corresponding deterministic system is transitioning from the B stability region to the M0 stability region through the co-dimension 2 bifurcation point. For low noisiness ($Y = 0.01Y^*$), the transition from BI=−1 to BI=0 is sharp, while as the noisiness is increased to $Y = 0.1Y^*$ and $Y = Y^*$, the transition becomes more gradual and occurs over a progressively larger range of X values. Thus, we can conclude that for true alternating activity bouts to occur, the corresponding determinstic system must be firmly within the B region, and that the lower the noisiness of the excitatory currents the closer the corresponding deterministic system can be to the boundary of the B region while still obtaining true bout behavior. In other words, the noisier the system, the closer the corresponding deterministic system must be to the center of the B region to elicit well-defined, alternating spike bouts.

In Fig. 11 (*left*), we see that for very low values of X (below $X =\sim 0.5$), the BI of the system rises as $X \to 0$. This occurs because for very low values of X, the corresponding deterministic system is in the $\alpha_1, \alpha_2 < g$ regime (i.e., in the regime where excitation is insufficient to allow either neuron to spike). Thus, in the noisy system, the mean of the excitatory currents keeps the membrane potential of the two neurons below threshold, and one of the neurons will spike only when a transient positive fluctuation in its excitatory current pushes its membrane potential above the spike

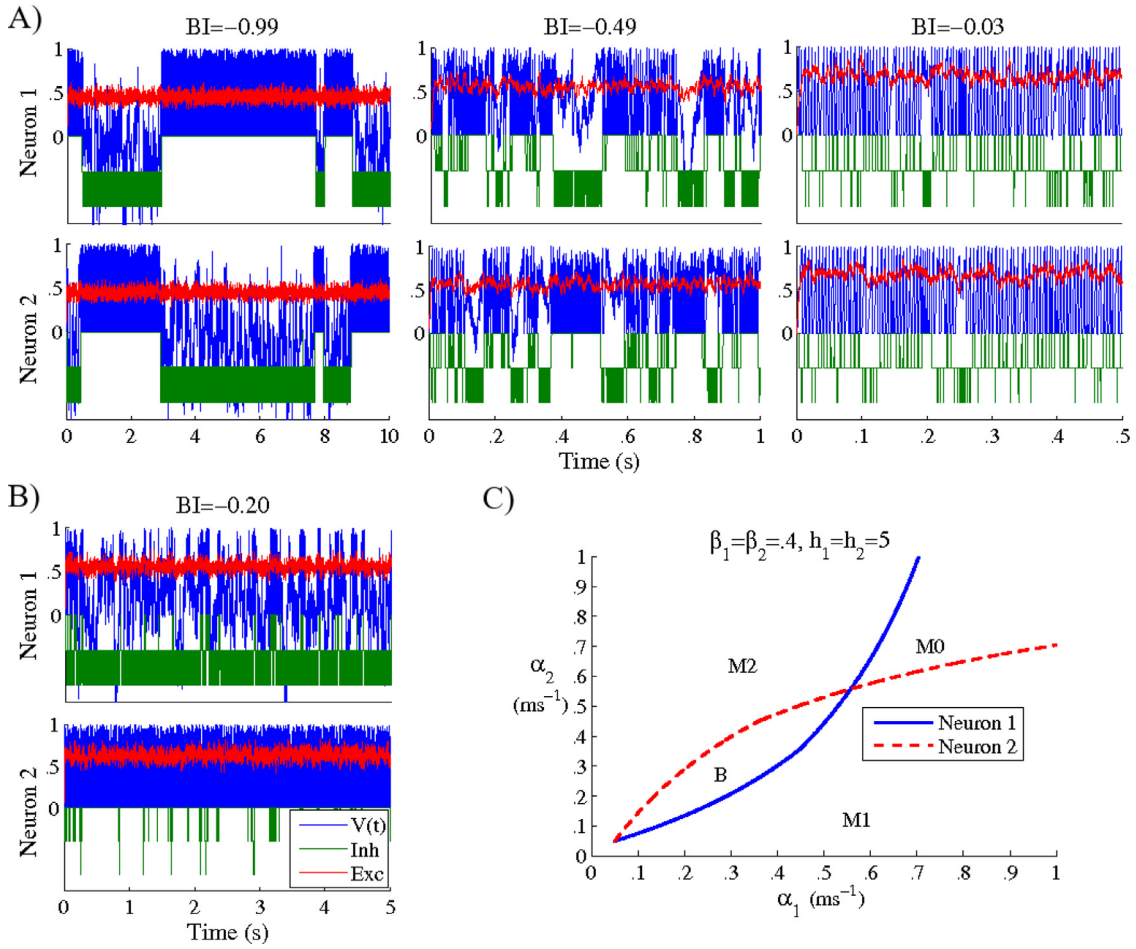

Fig. 10. Spiking activity and *bout index* (BI) of the two-neuron system with noisy excitatory currents (see text for details). *A)* Spiking activity of the two neurons when the corresponding deterministic system is in the B0 regime (left; $X_1 = X_2 = 2X^*$), at the co-dimension 2 bifurcation (middle; $X_1 = X_2 = 2.5X^*$), or within the M0 regime (right; $X_1 = X_2 = 3X^*$). The noisiness of the excitatory currents is fixed at $Y_1 = Y_2 = 0.01Y^*$. *B)* Spiking activity of the two neurons when the corresponding deterministic system is within the M2 regime ($X_1 = 2.5X^*$, $X_2 = 2.8X^*$; $Y_1 = Y_2 = 0.01Y^*$). *C)* Stability diagram of the corresponding deterministic system in the α_1, α_2 plane. The co-dimension 2 bifurcation occurs at $\alpha_1 = \alpha_2 = \sim 0.55$.

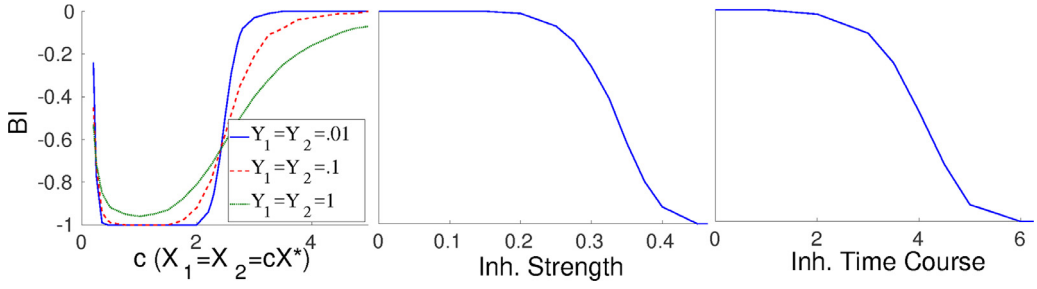

Fig. 11. *Bout index* (BI) of the two-neuron system with noisy excitatory currents (see text for details). In the left panel, the BI of the system is plotted as a function of the strength X of the noisy excitatory currents to the two neurons for different fixed values of the noisiness Y. In the middle and right panels, the statistics of the noisy excitatory currents are fixed and the BI of the system is plotted as either the amplitude β or time course h of synaptic inhibition are symmetrically varied, respectively. Left: $\beta_1 = \beta_2 = 0.4$, $h = h_1 = h_2 = 5$; Middle: $X_1 = X_2 = 2X^*$, $Y_1 = Y_2 = .1Y^*$, $h_1 = h_2 = 5$; Right: $X_1 = X_2 = 2X^*$, $Y_1 = Y_2 = .1Y^*$, $\beta_1 = \beta_2 = .4$.

threshold. Spiking is therefore rare and sporadic, and the spiking of neuron j is controlled not by inhibition from the other neuron but primarily by fluctuations in its own excitatory current. This results in a lack of correlation between the spiking activity of the two neurons, with the correlation between the activity of the two neurons declining as $X \to 0$ and spikes become progressively more scarce, yielding a BI that approaches 0.

In the other panels of Fig. 11, we fix the strength $X = X_1 = X_2$ and noisiness $Y = Y_1 = Y_2$ of the noisy excitatory currents and plot the BI of the system as either the amplitude $\beta = \beta_1 = \beta_2$ (Fig. 11; *middle*) or time course $h = h_1 = h_2$ (Fig. 11; *right*) of inhibition is varied. As either β or h is increased, the BI of the system falls from 0 to -1. For weak inhibition, neither neuron can silence the other, and both neurons tend to spike concurrently and nearly independent of each other ($\mathrm{BI} \to 0$), while when inhibition is strong (relative to excitation), each neuron is capable of quieting the other and the system exhibits alternating bouts of activity ($\mathrm{BI} \to -1$). This can also be inferred from the stability diagrams in the α_1, α_2 plane shown in Fig. 6 – as inhibition is strengthened, the B stability region appears and grows larger; hence, given a point *a, b* in the M0 region of the α_1, α_2 plane, as inhibition is strengthened the B stability region will eventually encompass *a, b*.

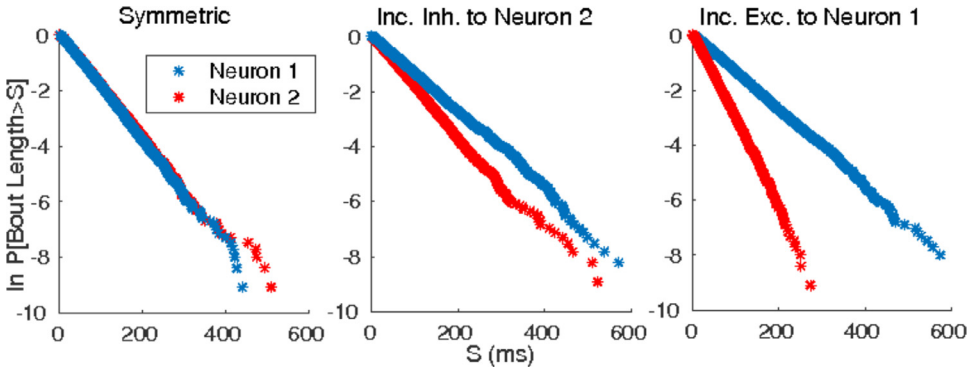

Fig. 12. Bout distributions of the current-based integrate-and-fire two-neuron system with noisy excitatory currents when the corresponding deterministic system is in the B stability regime. The left, middle, and right panels show P[Bout Length > S] vs. S with a log scale on the *y*-axis in the case that parameters for the two neurons are symmetric, inhibition from neuron 1 to neuron 2 is increased, and the noisy excitation to neuron 1 is increased, respectively. The linear relationships indicate exponential distributions. The mean bout times for neuron 1 and neuron 2 are: 57 ms and 57 ms (left), 77 ms and 58 ms (middle), 77 ms and 35 ms (right). Left: $\beta_1 = \beta_2 = 0.4$, $h_1 = h_2 = 5$, $X_1 = X_2 = 2X^*$, $Y_1 = Y_2 = Y^*$. Middle: β_2 changed to 0.45. Right: X_1 changed to $2.25X^*$. Data are collected over a 1000 s run with at least 5000 bouts per neuron.

5. Discussion

In this work, we used analytic and computational tools to examine monostability versus bistability in a system of two mutually inhibitory neurons being driven by constant excitatory currents, using two neuron models (the voltage-based and current-based integrate-and-fire models). Analytically, we found 3 possible monostable regimes and 1 possible bistable regime: (1) both neurons spike simultaneously for all time (M0); (2) neuron 1 fires with neuron 2 silent (M1); (3) neuron 2 fires with neuron 1 silent (M2); (4) one neuron fires with the other quiet, with the identities of the active and passive cells determined by the initial conditions (B). We found that these stability regimes encompass all possible behavior for the voltage-based integrate-and-fire model, but interestingly for the integrate-and-fire model two additional bistable regimes and a tristable regime may exist: (5) either neuron 1 fires with neuron 2 silent or both neurons spike concurrently (B1); 6) either neuron 2 fires with neuron 1 silent or both neurons spike concurrently (B2); 7) either neuron 1 fires with neuron 2 silent, neuron 2 fires with neuron 1 silent, or both neurons spike concurrently (T). However, we found that obtaining B1, B2, or T behavior requires delicate fine-tuning of parameters, suggesting that these regions may not be as important physiologically. The set of all possible stability regimes is described in Table 1. Furthermore, we found that synaptic inhibition exerts *independent control* over the spiking versus quiescence behavior of the two neurons, in the sense that inhibition from neuron *j* to neuron *k* only affects the behavior of neuron *k* (and has no impact on the behavior of neuron *j*). Excitation, on the other hand, exerts no such independent control – the excitatory current to neuron *j* influences the behavior of *both* neuron *j* and neuron *k*.

Finally, we examined the behavior of the system in the case that the excitatory currents to the two neurons were allowed to be noisy; in this case, if the corresponding deterministic system is in the M0 regime, then in the noisy system the two neurons will fire nearly independent of each other, while if the corresponding deterministic system is in the B regime, then in the noisy system the two neurons will exhibit alternating bouts of activity. We devised a metric we termed the *bout index* (BI) to assess behavior in the stochastic case, and, as system parameters are varied, we found that the system transitions from concurrent spiking to bout behavior in agreement with the stability diagrams of the corresponding deterministic system. Moreover, we found that the sharpness of the transition is inversely related to the noisiness of the excitatory currents within the system.

5.1. Choice of model

In this study, we modeled our two cells as voltage-based integrate-and-fire neurons (with instantaneous input) or current-based integrate-and-fire neurons (with temporally structured input) that receive constant or noisy excitatory currents and inhibit each other synaptically. We chose such simplified models because of their analytical tractability – the models allowed us to explicitly derive Poincare maps or suppression conditions for the two neurons and plot stability diagrams. In fact, the {B1, B2, T} stability regimes, which are difficult to derive analytically, could be found computationally only because of precise knowledge about the location of the co-dimension 2 bifurcation point in the stability diagrams obtained through analytical calculations. Furthermore, in our analysis we found that the {B1, B2, T} stability regimes do not exist in the voltage-based integrate-and-fire model, but are present only in the current-based integrate-and-fire model. This is a consequence of the temporal dynamics of inhibition – in the voltage-based integrate-and-fire model, inhibitory synapses between the two neurons are instantaneous (inhibitory inputs are modeled as delta functions), while in the current-based integrate-and-fire model inhibition from one neuron to the other has a finite time course. Moreover, in the current-based integrate-and-fire model we found that the B*j* stability region exists only when $h_j > T_k$ $(j \neq k \in \{1, 2\})$, where h_j is the time course of inhibition to neuron j and T_k is the interspike interval of neuron k, while the T stability region exists only when both $h_1 > T_2$ and $h_2 > T_1$ (as explained in the *Other Stability Regimes* section). In the voltage-based integrate-and-fire model, since inhibitory input is instantaneous, these conditions cannot be satisfied, and hence the {B1, B2, T} stability regimes are precluded from occurring. Thus, while the voltage-based model exhibits greater analytic tractability than the current-based integrate-and-fire model, the lack of inhibitory temporal dynamics has significant dynamical consequences – the voltage-based model is unable to capture the dynamics associated with the {B1, B2, T} stability regimes. This underscores the importance of model selection – the full dynamics of network behavior may not emerge if the neuron model is simplified to neglect the temporal dynamics of synaptic transmission, as in the voltage-based model, though the basic stability behavior described by the {M0, M1, M2, B} regimes can still be investigated with such a model.

While the quantitative results presented in this paper are specific to our particular model choices, the qualitative results are generally applicable. It is reasonable to expect in general that a pair of reciprocally inhibitory neurons, with or without noise added to the excitatory driving currents, will exhibit the dynam-

ical behaviors and stability regimes described in this paper. Furthermore, the behavior of a pair of reciprocally inhibitory neurons may be applicable to the case of two mutually inhibitory populations of neurons. If the two populations strongly inhibit each other with relatively weak intra-population connectivity, we expect that similar general principles to those described in this paper will govern the behavior of the mutually inhibitory populations.

5.2. Sleep-Wake cycling

In particular, the results in this paper may provide a useful starting point for the study of sleep-wake cycling in infant mammals. Infant mammals cycle between the behavioral states of sleep and wakefulness, spending a random amount of time within each state. The durations of sleep or wake bouts are exponentially distributed random variables and both sleep and wake bouts exhibit no bout-to-bout memory (the duration of the current bout is statistically independent of the duration of prior bouts), with mean sleep and wake bout times increasing (while remaining exponentially distributed) through early infancy independently of each other (Blumberg et al., 2005; Gall et al., 2009; Halász et al., 2004; Karlsson et al., 2005; 2004; Kleitman and Engelmann, 1953; Lo et al., 2004; 2002). Behavioral sleep and wake states are each correlated with the activity of 'sleep-active' (e.g., nucleus pontis oralis cells) and 'wake-active' (e.g., dorsolateral pontine tegmentum cells) populations within the brain that may reciprocally inhibit each other. During a sleep bout, 'sleep-active' neurons fire and 'wake-active' neurons are quiet, while during a wake bout, 'wake-active' neurons fire and 'sleep-active' neurons are silent (Blumberg et al., 2005; Karlsson et al., 2005). This picture is reminiscent of stochastic switching within a bistable system; from a dynamical systems perspective, sleep and wakefulness represent two deterministically stable states of the system, with the two stable states given by spiking of one population and quiescence of the other.

Fig. 12 shows bout distributions of the current-based integrate-and-fire two-neuron system in the case that the corresponding deterministic system is within the B stability regime, with a log scale on the y-axis (the linear relationships indicate exponential bout distributions). The left panel shows the case where parameters are symmetric and mean bout times are equivalent for the two neurons – exponential bout distributions arise due to a lack of memory within the system (when one neuron is spiking, its mean spike rate is constant due to its constant-mean excitatory drive, indicating that the inhibition delivered to the other neuron approaches a steady state mean value on a time scale that is rapid relative to the time scale of bouts; along with the constant means of the noisy excitatory currents to the two neurons, this implies that there exists no vehicle via which the system can track the duration of an ongoing bout). The mean bout times of the two neurons can be modified by altering the strength of inhibition or the excitatory drive. Increasing the strength of inhibition from neuron 1 to neuron 2 increases the mean bout time of neuron 1 without affecting the mean bout time of neuron 2 (Fig. 12, middle), since inhibition from neuron 1 to neuron 2 is only active during a bout of neuron 1 (during a bout of neuron 2, neuron 1 is quiescent), and hence increasing the strength of neuron 1 to neuron 2 inhibition impacts only bouts of neuron 1. Increasing the strength of excitation to neuron 1, on the other hand, both increases the mean bout time of neuron 1 and decreases the mean bout time of neuron 2 (Fig. 12, right) – increased excitation to neuron 1 implies that when neuron 1 is in a bout, the probability of a bout switch is lowered, while when neuron 2 is in a bout, the probability of a bout switch is higher (since the increased excitation to neuron 1 implies that a smaller fluctuation is required for neuron 1 to initiate a bout switch). This suggests that stochastic switching in a bistable system may provide a natural explanation of sleep-wake switching through early infancy – constant-mean noisy excitation to sleep and wake populations naturally leads to exponential sleep and wake bout distributions, while inhibition between the two populations provides a method by which mean sleep and wake bout times can be independently regulated as the animal ages through early infancy. A comprehensive analysis of bout distributions within the context of sleep-wake switching is carried out in other work (Patel, 2015; Patel and Joshi, 2014; Patel and Rangan, 2017). The results presented in this paper may provide a foundation for understanding the nature of the reciprocal inhibition required to place two populations within the (deterministic) B regime, as well as assessing the bout behavior of the two populations when the system is permitted to be noisy.

References

Blumberg, M., Seelke, A., Lowen, S., Karlsson, K., 2005. Dynamics of sleep-wake cyclicity in developing rats. Proc. Natl. Acad. Sci. U.S.A. 102 (41), 14860.

Elson, R., Selverston, A., Abarbanel, H., Rabinovich, M., 2001. Inhibitory synchronization of bursting in biological neurons: dependence on synaptic time constant. J Neurophysiol 88. 1166–76

Friesen, W., 1994. Reciprocal inhibition: a mechanism underlying oscillatory animal movements. Neurosci. Biobehav. Rev. 18, 547–553.

Gall, A., Joshi, B., Best, J., Florang, V.R., Doorn, J.A., Blumberg, M., 2009. Developmental emergence of power-law wake behavior depends upon the functional integrity of the locus coeruleus. Sleep 32 (7), 920–926.

Halász, P., Terzano, M., Parrino, L., Bódizs, R., 2004. The nature of arousal in sleep. J. Sleep Res. 13 (1), 1–23.

Hobson, J., McCarley, R., Wyzinski, P., 1975. Sleep cycle oscillation: reciprocal discharge by two brainstem neuronal groups. Science 189 (4196), 55.

Jalil, S., Belykh, I., Shilnikov, A., 2010. Fast reciprocal inhibition can synchronize bursting neurons. Phys. Rev. E Stat. Nonlinear Soft Matter Phys. 81, 045201.

Karlsson, K., Gall, A., Mohns, E., Seelke, A., Blumberg, M., 2005. The neural substrates of infant sleep in rats. PLoS Biol. 3 (5), e143.

Karlsson, K., Kreider, J., Blumberg, M., 2004. Hypothalamic contribution to sleep--wake cycle development. Neuroscience 123 (2), 575–582.

Kirillov, A., Myre, C., Woodward, D., 1993. Bistability, switches and working memory in a two-neuron inhibitory-feedback model. Biol. Cybern. 68 441-9.

Kleitman, N., Engelmann, T., 1953. Sleep characteristics of infants. J. Appl. Physiol. 6 (5), 269–282.

Lo, C., Chou, T., Penzel, T., Scammell, T., Strecker, R., Stanley, H., Ivanov, P., 2004. Common scale-invariant patterns of sleep–wake transitions across mammalian species. Proc. Natl. Acad. Sci. U.S.A. 101 (50), 17545.

Lo, C., Nunes Amaral, L., Havlin, S., Ivanov, P., Penzel, T., Peter, J., Stanley, H., 2002. Dynamics of sleep-wake transitions during sleep. EPL (Europhys. Lett.) 57, 625.

Lu, J., Sherman, D., Devor, M., Saper, C., 2006. A putative flip–flop switch for control of rem sleep. Nature 441 (7093), 589–594.

Mysore, S., Knudsen, E., 2012. Reciprocal inhibition of inhibition: a circuit motif for flexible categorization in stimulus selection. Neuron 73 (1), 193–205.

Patel, M., 2015. A simplified model of mutually inhibitory sleep-active and wake-active neuronal populations employing a noise-based switching mechanism. J. Theor. Biol. 394, 127–136.

Patel, M., Joshi, B., 2014. Switching mechanisms and bout times in a pair of reciprocally inhibitory neurons. J. Comput. Neurosci. 36, 177–191. doi:10.1007/s10827-013-0464-6.

Patel, M., Rangan, A., 2017. Role of the locus coeruleus in the emergence of power law wake bouts in a model of the brainstem sleep-wake system through early infancy. J. Theor. Biol. 426, 82–95.

Rowat, P., Selverston, A., 1997. Oscillatory mechanisms in pairs of neurons connected with fast inhibitory synapses. J. Comput. Neurosci. 4 103-27.

Seely, J., Chow, C., 2011. Role of mutual inhibition in binocular rivalry. J. Neurophysiol. 106 2136-50.

Skinner, F., Kopell, N., Marder, E., 1994. Mechanisms for oscillation and frequency control in reciprocally inhibitory model neural networks. J. Comput. Neurosci. 1, 69–87.

Stein, R.B., 1965. A theoretical analysis of neuronal variability. Biophys. J. 5 (2), 173–194.

Tao, L., Shelley, M., McLaughlin, D., Shapley, R., 2004. An Egalitarian network model for the emergence of simple and complex cells in visual cortex. Proc. Natl. Acad. Sci. 101 366-71.

Terman, D., Kopell, N., Bose, A., 1998. Dynamics of two mutually coupled slow inhibitory neurons. Phys. D 117 241-75.

Van Vreeswijk, C., Abbott, L., Ermentrout, G., 1994. When inhibition not excitation synchronizes neural firing. J. Comput. Neurosci. 1 313-21.

Wang, X., Rinzel, J., 1992. Alternating and synchronous rhythms in reciprocally inhibitory model neurons. Neural Comput. 4, 84–97.